

DISCRETE MAXIMUM PRINCIPLE PRESERVING SCHEME FOR 1-D NONLOCAL
TO LOCAL DIFFUSION PROBLEM: DEVELOPMENT, ANALYSIS, AND
SIMULATION

by

Amanda Gute

A dissertation submitted to the faculty of
The University of North Carolina at Charlotte
in partial fulfillment of the requirements
for the degree of Doctor of Philosophy in
Applied Mathematics

Charlotte

2024

Approved by:

Dr. Ronald E. Smelser

Dr. Duan Chen

Dr. Kevin McGoff

Dr. Bei-Tseng Chu

©2024
Amanda Gute
ALL RIGHTS RESERVED

ABSTRACT

AMANDA GUTE. Discrete maximum principle preserving scheme for 1-D nonlocal to local diffusion problem: development, analysis, and simulation. (Under the direction of DR. RONALD E. SMELSER)

Diffusion is a scientific phenomena that can be modeled by partial differential equations. In this dissertation we first explore the development of equations for local, nonlocal, and quasi-nonlocal diffusion. Methods of finding solutions will be discussed as well as the properties of each diffusion model type. These properties include satisfying the maximum principle and demonstrating the well-posedness of each model which is through the solutions existence, uniqueness, and stability.

Also in a recent paper [15], a quasi-nonlocal coupling method was introduced to seamlessly bridge a nonlocal diffusion model with the classical local diffusion counterpart in a one-dimensional space. The proposed coupling framework removes interfacial inconsistency, preserves the balance of fluxes, and satisfies the maximum principle of the diffusion problem. However, the numerical scheme proposed in that paper does not maintain all of these properties on a discrete level. We resolve this issue by proposing a new finite difference scheme that ensures the balance of fluxes and the discrete maximum principle. We rigorously prove these results and provide the stability and convergence analyses accordingly. In addition, we provide the Courant-Friedrichs-Lewy (CFL) condition for the new scheme and test a series of benchmark examples which confirm the theoretical findings.

ACKNOWLEDGEMENTS

I would like to thank my advisor Dr. Ronald E. Smelser, Co-Chair Dr. Duan Chen, and committee members Dr. Kevin McGoff, and Dr. Bei-Tseng (Bill) Chu, with special thanks to Dr. Oleg Safranov, Dr. Hae-Soo Oh, Dr. Mohammad Kazemi, and Dr. Taufiqar Khan.

I would also like to acknowledge the financial support I received through research funding provided by Dr. X. Li who is supported by an NSF CAREER award: DMS-1847770 and the University of North Carolina at Charlotte Faculty Research Grant. Also other funding was provided by a Graduate School Summer Fellowship Grant (GSSF), Graduate Assistant Support Plan (GASP), and various travel grants from American Mathematical Society (AMS), University of North Carolina at Charlotte, Graduate and Professional Student Government (GPSG), and the University of North Carolina at Charlotte Mathematics Department.

Finally I would like to thank my family for their support through a very long academic journey, my kids for sacrificing time with their mom, and most of all my husband who has sat next to me and supported me in school since the first grade.

TABLE OF CONTENTS

v

LIST OF TABLES	vi
LIST OF FIGURES	vii
CHAPTER 1: INTRODUCTION	1
1.1. Local Diffusion	2
1.2. Nonlocal Diffusion	5
1.3. Coupling Nonlocal and Local Diffusion	9
CHAPTER 2: FINITE DIFFERENCE SCHEME FOR QNL COUPLING	20
2.1. Discretized Quasi-Nonlocal Coupling	22
2.2. Consistency of the Discretized Quasi-Nonlocal Operator	26
2.3. Stability of the Discretized Quasi-nonlocal Operator	32
2.4. Convergence of Discretized Quasi-nonlocal Operator	40
2.5. Study of the Courant-Friedricks-Lewy (CFL) Condiditon	42
2.6. Numerical Examples	46
2.7. New Finite Difference Scheme Conclusion	49
CHAPTER 3: DEVELOPMENT OF THE COEFFICIENT MATRIX, AND MORE NUMERICAL EXAMPLES	50
3.1. Numerical Constants	53
3.2. Neumann Boundary Conditions Numerical Example	59
3.3. Robin Boundary Conditions Numerical Example	62
3.4. Boundary Conditions Conclusion	64
REFERENCES	65

- TABLE 2.1: $L_{\Omega \times [0, T]}^\infty$ differences between the local continuous solution u^ℓ and discrete solution $u_{\delta, \Delta x}^{qnl}$. We fix $\delta = 3\Delta x$, and the kernel is $\gamma_\delta(s) = \frac{3}{\delta^3} \chi_{[-\delta, \delta]}(s)$. The termination time $T = 1$ and $\Delta t = 0.2\Delta x^2$. 47
- TABLE 2.2: $L_{\Omega \times [0, T]}^\infty$ differences between the local continuous solution u^ℓ and two discrete solutions $u_{\delta, \Delta x}^{qnl}$, $\tilde{u}_{\delta, \Delta x}^{qnl}$ using the FDM schemes (2.6) and (2.8), respectively. We fix $\delta = 3\Delta x$, and the kernel is $\gamma_\delta(s) = \frac{3}{\delta^3}$. The termination time is $T = 1$ and $\Delta t = 0.2\Delta x^2$. 48
- TABLE 3.1: $L_{\Omega \times [0, T]}^\infty$ differences between the local continuous solution u^ℓ and discrete solution $u_{\delta, \Delta x}^{qnl}$. We fix $\delta = 3\Delta x$, and the kernel is $\gamma_\delta(s) = \frac{3}{\delta^3} \chi_{[-\delta, \delta]}(s)$. The termination time $T = 1$ and $\Delta t = 0.2\Delta x^2$. 62
- TABLE 3.2: $L_{\Omega \times [0, T]}^\infty$ differences between the local continuous solution u^ℓ and discrete solution $u_{\delta, \Delta x}^{qnl}$. We fix $\delta = 3\Delta x$, and the kernel is $\gamma_\delta(s) = \frac{3}{\delta^3} \chi_{[-\delta, \delta]}(s)$. The termination time $T = 1$ and $\Delta t = 0.2\Delta x^2$. 64

FIGURE 1.1: Diffusion flow of particles from higher concentration to lower concentration.	3
FIGURE 1.2: Domain body of the diffusion problem.	4
FIGURE 1.3: The maximum of the solution is initially, or on the boundaries.	5
FIGURE 1.4: Partitioning and boundary layer for a one dimensional domain.	12
FIGURE 2.1: Partitioning and boundary layer for a discretized one dimensional domain.	22
FIGURE 2.2: Example finite difference stencil with $\Delta x = \frac{1}{5}$, horizon $\delta = r\Delta x$, and $r = 3$.	25
FIGURE 2.3: Maximum Growth Rate of (2.58), (2.59), (2.60) for the new finite difference method versus that of (2.8) for the original finite difference method.	45
FIGURE 2.4: Plots of solutions to the approximate and actual solutions. The kernel function was chosen as $\gamma_\delta(s) = \frac{3}{\delta^3}\chi_{[-\delta,\delta]}(s)$. The coupling inference is at $x^* = 0$, and the mesh size is $\Delta x = \frac{1}{400}$ with a horizon as $\delta = \frac{3}{400}$, the temporal step size is $\Delta t = 0.45\Delta x^2$.	47
FIGURE 2.5: Numerical comparison between the new scheme (2.6) and original scheme (2.8) used to approximate (2.72) with external force given by (2.73). The spatial step size is $\Delta x = \frac{1}{200}$ and $\Delta t = 0.25\Delta x^2$.	49
FIGURE 3.1: Numerical comparison between approximate and actual solution with Neumann Boundary Conditions	61
FIGURE 3.2: Numerical comparison between approximate and actual solution with Robin Boundary Conditions	63

CHAPTER 1: INTRODUCTION

Diffusion may not be a novel concept, but it underpins many research fields that analyze the movement of various mediums using fundamental mathematical processes. The primary forms of diffusion are local and nonlocal diffusion. Local diffusion is widely studied and has diverse applications. It relies on cohesive materials, allowing for uninterrupted communication between points, which facilitates quick and straightforward numerical solutions. Research on local diffusion spans a range of areas, including geology, energy, neuroscience, cancer studies, and the movement of people and ideas [34] [48] [10] [7].

Nonlocal diffusion is a more recent model that addresses how something spreads in scenarios where the space is not cohesive. It accounts for disconnections in ideas, material flaws, or other singularities. While nonlocal diffusion can be used interchangeably with local diffusion, it typically requires more time for numerical solutions. Nevertheless, its ability to minimize imperfections keeps it in demand. Research employing nonlocal diffusion can be found in fields such as geology, imaging, machine learning, and mechanics, among others [8] [22] [38] [6] [13] [41]. Given the time constraints associated with numerically solving nonlocal models, there is a growing need to couple nonlocal and local models, a concept that will be explored in greater detail throughout this dissertation.

We will start by examining the continuous model of local diffusion and its beneficial properties. Next, we will provide a review of the continuous model for nonlocal diffusion. After outlining these two models, we will discuss the necessity of a coupling operator to connect nonlocal and local diffusion models. This will include the development of a specific coupling operator, which will then be discretized for use in numerical approximation experiments and analysis.

Next, we will introduce a finite difference numerical discretization scheme that closely aligns with a previously developed approach but incorporates an essential property of the discretized maximum principle. This addition ensures guaranteed convergence of the approximate solution provided by this new finite difference scheme for the given quasi-nonlocal coupling operator. After presenting the finite difference scheme, the sections focus on proving its consistency, stability, and convergence. In the subsequent section, we will briefly analyze the Courant-Friedrichs-Lewy (CFL) condition and provide benchmark examples to further validate our results. We will conclude with a comparison of the approximation results from the previous scheme and the new scheme.

The final chapter begins by deriving the numerical local to nonlocal operator from the continuous local to nonlocal operator of the diffusion problem under Dirichlet boundary conditions. We then develop the coefficient matrix for the numerical operator, addressing Dirichlet, Neumann, and Robin boundary conditions. Following this, we provide benchmark examples to evaluate the performance of the developed numerical local to nonlocal diffusion operator under Neumann and Robin boundary conditions. Finally, we compare the results of the numerical local to nonlocal finite difference scheme across all three types of boundary conditions.

1.1 Local Diffusion

Diffusion is a widely studied topic that has generated significant insights and research across various fields. Essentially, diffusion refers to the process of spreading out, and it encompasses important concepts in several seemingly unrelated areas. Examples of diffusion include the movement of atoms, particles, people, animals, ideas, and prices, all of which are extensively explored in disciplines such as physics, chemistry, biology, sociology, economics, and finance.

Diffusion is a phenomenon where the rate of diffusion is proportional to the negative gradient of concentration. This implies that particles move from regions of higher concentration to regions of lower concentration, heat transfers from hotter to cooler areas, or people migrate

from more populated to less populated regions, ultimately leading to a uniform distribution of the diffusing substance (see an illustration in Figure 1.1). Mathematically, this behavior can be described using parabolic equations derived from Fick's second law.

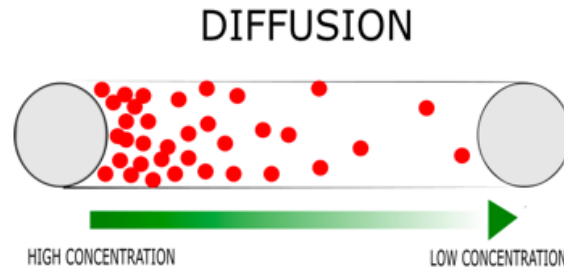


Figure 1.1: Diffusion flow of particles from higher concentration to lower concentration.

Proposition 1 (Fick's Second Law, [2]). *Fick's second law is a partial differential equation defined as*

$$u_t(x, t) = Du_{xx}(x, t), \quad (1.1)$$

where u is concentration, and D is the diffusion coefficient. The solution $u(x, t)$ that satisfies this partial differential equation predicts how diffusion causes the concentration to change with respect to space and time.

A physical interpretation of Fick's second law is that u_{xx} represents the difference between the average value of the function in the vicinity of a point and its value at that specific point. For instance, if $u(x, t)$ represents the concentration, then u_{xx} describes how the average density in the surrounding region differs from the density at that point.

We recall the well-posedness of the local diffusion model when the initial and boundary conditions are specified.

Theorem 1 (The existence, uniqueness, and stability, see [36]). *Let f be a function in $L^\infty(0, L)$, and let g and h be functions in $L^\infty(0, T)$. Then, the following problem:*

$$\begin{cases} u_t(x, t) = Du_{xx}(x, t) & (x, t) \in R \\ u(x, 0) = f(x) & x \in (0, L) \\ u(0, t) = h(t) & t \in (0, T) \\ u(L, t) = g(t) & t \in (0, T) \end{cases} \quad (1.2)$$

has a unique solution. Moreover, if $f_1, f_2 \in L^2(0, L)$ and $g_1, g_2, h_1, h_2 \in L^2(0, T)$, and let u_1 and u_2 be the solutions to (1.2) corresponding to the initial data f_1, f_2 and boundary data g_1, g_2 and h_1, h_2 , respectively, then

$$\|u_1 - u_2\|_{L^\infty(R)} \leq \max \{ \|f_1 - f_2\|_{L^\infty(0, L)}, \|g_1 - g_2\|_{L^\infty(0, T)}, \|h_1 - h_2\|_{L^\infty(0, T)} \}.$$

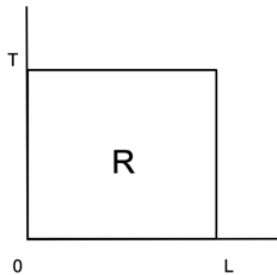


Figure 1.2: Domain body of the diffusion problem.

We will now recall a well-known property of the general solution to the diffusion problem, referred to as the *Maximum Principle Property*. In this scenario, the function u represents the temperature distribution over the interval $[0, L]$, with time t ranging within $[0, T]$. Let $R = [0, L] \times [0, T]$ (see Figure 1.2). Physically, as the temperature diffuses over time, the maximum temperature within R will occur either at the initial time or at the endpoints 0 and

L . No new extreme values will arise within the interior $(0, L)$ as time progresses. In Figure 1.3, the locations where u attains its maximum values are marked in red. The Maximum Principle is stated below. Its proof can be found in many textbooks of PDEs, for e.g., [36].

Theorem 2 (Maximum Principle for the Local Diffusion Equation, see [36]). *If $u(x, t)$ satisfies the diffusion equation (1.1) in R then the maximum value of $u(x, t)$ over R is either initially, or on the boundaries.*

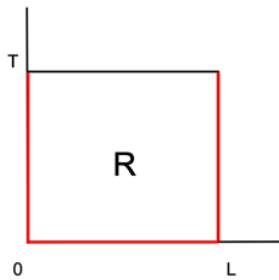


Figure 1.3: The maximum of the solution is initially, or on the boundaries.

In this dissertation, we develop a numerical scheme based on finite difference methods to compute solutions for a "combined" local and nonlocal diffusion model. Existing finite difference schemes for this problem, [15], may not satisfy the Maximum Principle, whereas our approach does, which is the primary reason for revisiting the Maximum Principle here. As previously mentioned, our study involves a nonlocal model. For completeness, we will review the relevant nonlocal equations and some of their properties in the following section.

1.2 Nonlocal Diffusion

The following discussions draw upon references such as [3], [26], [1], [39], [44], [9], [18], [42], [40], [17], and [13].

The nonlocal diffusion problem largely originates from the nonlocal continuum theory known as peridynamics, which addresses the formulation of governing equations that can be applied at discontinuities. Unlike traditional local partial differential equations, which rely on spatial

derivatives that become undefined at discontinuities, nonlocal models replace these derivatives with integral expressions that remain well-defined. This approach enables nonlocal models to accurately handle singularities and discontinuities by using integral operators, which provide a framework to account for these irregularities in a structured manner, allowing for them to be bypassed or treated through a vanishing property.

The vanishing property arises from the inclusion of a kernel function in the nonlocal model, which is defined based on a chosen horizon, denoted as δ . The horizon represents the effective range over which nonlocal interactions occur. As $\delta \rightarrow 0$, the nonlocal model converges to the local model. The radius of the horizon is determined by the values that establish the null space within the domain, allowing the solutions to be averaged over this region. Within the specified ball, the solutions effectively vanish at singularities, facilitating the treatment of discontinuities in the model.

Nonlocal diffusion can be interpreted as the evolution of a Gaussian distribution, where the solution changes over time by increasing at points where the mean value is higher than the current value, and decreasing when the mean value is lower [39]. A commonly used formulation for modeling nonlocal diffusion is given by

$$u_t(x, t) = \int_{\mathbb{R}} J(x - y)(u(y, t) - u(x, t)) dy,$$

where $J : \mathbb{R} \rightarrow \mathbb{R}$ is a nonnegative, smooth function that satisfies $\int_{\mathbb{R}} J = 1$ [3].

In contrast to the basic local diffusion model, which requires only the value of u at point x for evaluating u_{xx} , the nonlocal model requires the values of u at other points $y \neq x$ to compute the behavior at x . This dependency on values across a broader range enables the nonlocal approach to capture more complex interactions and account for discontinuities.

Consider the nonlocal Dirichlet boundary value problem defined as

$$\begin{cases} u_t(x, t) = \int_{\mathbb{R}} J(x - y)(u(y, t) - u(x, t))dy \\ u(x, 0) = u_0(x) \\ u(0, t) = u(L, t) = 0 \end{cases}$$

where $x \in \Omega = [0, L]$, and $t > 0$. Then the solution is the function

$$u(x, t) = u_0(x) + \int_0^t \int_{\mathbb{R}} J(x - y)(u(y, s) - u(x, s))dyds \quad (1.3)$$

where $u \in C([0, \infty); L^1(\mathbb{R}))$.

When studying the nonlocal diffusion problem, it is essential to ensure that a solution exists, is unique, and remains stable over time, as these properties are crucial for both the theoretical understanding and practical applications of the model.

The existence of a solution guarantees that the mathematical model accurately describes a real-world process. For the nonlocal diffusion equation, this means that the integral equation governing the diffusion process has at least one function that satisfies the equation under the given initial and boundary conditions. Proving the existence of a solution typically involves demonstrating that the integral operator in the nonlocal equation, such as $u_t(x, t) = \int_{\mathbb{R}} J(x - y)(u(y, t) - u(x, t))dy$, can map an initial state to a well-defined solution function. This is often achieved using mathematical techniques like fixed-point theorems or energy estimates.

Uniqueness of the solution ensures that the nonlocal diffusion problem has only one solution that satisfies the given initial and boundary conditions. Without uniqueness, the model would be ambiguous, leading to multiple interpretations of the physical phenomenon being studied. To prove uniqueness, it is typically shown that if two different solutions exist, then

the difference between them must be zero for all points in space and time. This is often accomplished using properties of the integral operator and the smoothness of the kernel function J , which helps control the behavior of the solutions.

Stability of the solution refers to its sensitivity to small changes in the initial or boundary conditions. A stable solution will exhibit only small variations in response to such perturbations, ensuring that the model's predictions are robust and reliable. Stability is particularly important when performing numerical simulations, where small errors can arise from discretization or rounding. If the solution is stable, these errors will not grow uncontrollably over time. To establish stability, it is common to examine the norm of the difference between two solutions with slightly different initial conditions and show that this norm does not significantly increase as time progresses.

These properties—existence, uniqueness, and stability—are important because they ensure that the nonlocal diffusion model behaves predictably and can be used to describe complex physical systems reliably. Existence guarantees that a solution can be found, uniqueness ensures that the solution is meaningful and interpretable, and stability provides confidence in the model's robustness to small changes. Together, these qualities make the nonlocal diffusion model a valuable tool for modeling materials with micro-cracks, anomalous diffusion, and other processes involving long-range interactions.

Theorem 3 (Uniqueness and Existence, see [3]). *The solution for the nonlocal diffusion Dirichlet boundary value problem is given by*

$$u(x, t) = u_0(x) + \int_0^t \int_{\mathbb{R}} J(x - y)(u(y, s) - u(x, s)) dy ds \quad (1.4)$$

where $u_0(x)$ represents the initial condition, and $J(x - y)$ is a nonlocal interaction kernel. The problem asserts that this solution exists and is unique for any initial condition $u_0(x) \in L^1(\Omega)$, where $L^1(\Omega)$ denotes the space of integrable functions over the domain Ω .

Theorem 4 (Stability, see [3]). *The solution $u(x, t)$ to the nonlocal homogeneous Dirichlet boundary value problem is stable for the initial condition $u_0 \in L^2(\Omega)$.*

Throughout the remainder of this dissertation, the nonlocal boundary value problem will be formulated using the nonlocal operator to account for nonlocal effects, thereby capturing interactions that extend beyond the immediate spatial location. This approach allows us to model phenomena where the behavior at a given point depends not only on local conditions but also on the influence of surrounding regions, which is critical in describing processes such as anomalous diffusion, long-range interactions in materials, or systems with memory effects. The use of the nonlocal operator provides a more general framework than classical differential operators, enabling a more comprehensive analysis of such complex systems.

$$\begin{cases} u_t(x, t) = \mathcal{L}u(x, t) \\ u(x, 0) = f(x) \\ u(0, t) = u(L, t) = 0 \end{cases}$$

This version smoothly introduces the nonlocal diffusion operator, setting up a transition to its formal definition used in this research.

Definition 1 (Nonlocal Diffusion Operator, see [23]).

$$\mathcal{L}u(x, t) = \int_{-\delta}^{\delta} \gamma(s)(u(x + s, t) - u(x, t))ds. \quad (1.5)$$

In the following section, we will discuss the coupling of nonlocal and local diffusion, exploring how these two mechanisms can be combined to model systems that exhibit both short-range and long-range interactions.

1.3 Coupling Nonlocal and Local Diffusion

Nonlocal modeling can be applied to solve even classical local diffusion problems, though it is computationally expensive. In many cases, singularities and discontinuities in the solution

can be isolated, allowing for a more efficient computational strategy. Specifically, the domain can be partitioned so that nonlocal models are used only in regions where they are essential, while local partial differential equations (PDEs) are applied in the rest of the domain. This hybrid approach, combining local and nonlocal models, has emerged as a promising solution to the high computational cost associated with using purely nonlocal models. Additionally, it helps address the complexities that arise from nonlocal boundary conditions, which can be difficult to manage in purely nonlocal frameworks.

By blending local and nonlocal methods, it is possible to maintain the accuracy and physical relevance of nonlocal models where needed, while leveraging the simplicity and computational efficiency of local PDEs in regions where nonlocal effects are negligible. This method not only reduces the overall computational load but also helps resolve boundary issues more effectively.

The discussion in this chapter draws from a variety of foundational texts that cover both the theory and practical implementation of local-to-nonlocal models, including works such as [29], [18], [23], [12], [28], [30], [31], and [15]. These texts provide a comprehensive understanding of the challenges and advancements in nonlocal modeling and its integration with local methods.

There are several categories of approaches to coupling local and nonlocal diffusion models, including generalized domain decomposition, atomistic-to-continuum coupling, energy-based methods, and force-based methods. The research presented in this dissertation focuses on the atomistic-to-continuum methodology, which is particularly well-suited for modeling systems that require a seamless transition between microscopic (atomistic) and macroscopic (continuum) behaviors.

In atomistic-to-continuum coupling, the local and nonlocal diffusion models are linked through a transition region where the two domains do not overlap. This approach allows for a smooth transition between the local and nonlocal regions, maintaining the integrity of the solution

across the boundary between the two domains. This is typically achieved by enforcing conservation laws, such as the conservation of energy, to ensure that the total energy of the system is preserved across both the local and nonlocal regions.

By using this coupling methodology, it becomes possible to capture the fine-scale behavior of materials in regions where nonlocal effects are significant, while using the more computationally efficient local models where nonlocal interactions are less important. This hybrid method addresses the challenges of computational cost and complexity that arise when using purely nonlocal models, providing a balanced and efficient solution for many physical problems.

The atomistic-to-continuum approach has proven effective in various applications, including materials science and mechanics, where the detailed atomistic behavior in localized regions influences the overall macroscopic behavior of the system.

Figure 1.4 illustrates the decomposition of the domain into distinct regions: nonlocal, transitional, local, and boundary, respectively. The overall domain is defined as $\Omega = [-1 - \delta, 1]$, with the subdomains described as follows:

- The **computational nonlocal boundary layer** $\Omega_\delta = [-1 - \delta, -1]$
- The **nonlocal region** is $\Omega_{NL} = (-1, 0)$,
- The **transitional region** is $\Omega_T = [0, \delta)$,
- The **local region** is $\Omega_L = [\delta, 1)$
- The **boundary region** is $\Omega_B = \{-1\} \cup \{1\}$.

The entire domain is the union of these regions, expressed as $\Omega = \Omega_{NL} \cup \Omega_T \cup \Omega_L \cup \Omega_B$. Ω represents the domain of the continuous model, but as seen in Figure 1.4, there's an additional region outside this domain, Ω_δ that must be accounted for to initialize the numerical model. This introduces a nonlocal boundary condition in the numerical approach. However,

as δ approaches 0, this nonlocal numerical boundary condition converges to the standard boundary condition of the continuous model. This ensures that, in the limit, the numerical solution matches the behavior of the continuous model at the boundary.

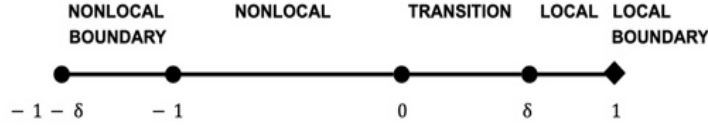


Figure 1.4: Partitioning and boundary layer for a one dimensional domain.

Here, δ , referred to as the **horizon**, plays a critical role in controlling the extent of nonlocal interactions. It is scaled to determine the effective interaction range that is required to capture the essential features of the solution, such as singularities and discontinuities, within the nonlocal region. The transitional region Ω_T serves as a smooth interface where the nonlocal and local models connect, ensuring that the solution transitions seamlessly between the different regions without overlap.

Next we will discuss the kernel function used to couple the nonlocal and local diffusion models. The choice of kernel is critical, as it governs the interaction strength between points within the nonlocal region and influences the smoothness and accuracy of the transition between the nonlocal and local domains. By carefully selecting and analyzing the kernel, we can ensure that the coupling effectively captures the essential features of both diffusion processes while maintaining stability and consistency across the entire domain.

Definition 2 (Nonlocal diffusion kernel, see [15]). *The nonlocal diffusion kernel $\gamma_\delta(x)$ is defined as*

$$\begin{cases} \gamma_\delta(|x|) = \frac{1}{\delta^3} \gamma\left(\frac{|x|}{\delta}\right), & \gamma \text{ is nonnegative and nonincreasing on } (0, 1), \\ \text{with } \text{supp}(\gamma) \subset [0, 1] \text{ and } \int_{\mathbb{R}} |x|^2 \gamma(|x|) dx = 1. \end{cases}$$

To effectively couple nonlocal and local diffusion, we must examine the energy equations for both models and formulate a combined energy framework. This involves integrating the energy contributions from the nonlocal and local regions, ensuring the total energy is conserved across the transition between the two. A key element in this process is the introduction of a weight function, which must possess specific characteristics to balance the contributions from both the nonlocal and local regions. The weight function will dictate the influence of each model in the transitional region, allowing for a smooth blending of the two diffusion processes while preserving the physical properties of the system.

Corollary 1 (See, [15]). *Given the definition of the weight function as*

$$\omega_\delta(x, t) = \int_0^1 dt \int_{|s| < \frac{x}{t}} |s|^2 \gamma(|s|) ds \quad (1.6)$$

then it is equal to

$$\omega_\delta(x, t) = 2 \int_0^x s^2 \gamma_\delta(|s|) ds + 2x \int_x^\infty s \gamma_\delta(|s|) ds, \quad (1.7)$$

and its derivative is

$$\omega'_\delta(x, t) = 2 \int_x^\infty s \gamma_\delta(s) ds. \quad (1.8)$$

Proof. By definition the weight function is

$$\omega_\delta(x, t) = \int_0^1 dt \int_{|s| < \frac{x}{t}} |s|^2 \gamma(|s|) ds. \quad (1.9)$$

By symmetry of the absolute value

$$\int_0^1 dt \int_{|s| < \frac{x}{t}} |s|^2 \gamma(|s|) ds = 2 \int_0^1 dt \int_0^{\frac{x}{t}} s^2 \gamma_\delta(|s|) ds. \quad (1.10)$$

Then with careful restructuring, we find

$$\begin{aligned}
2 \int_0^1 dt \int_0^{\frac{x}{t}} s^2 \gamma_\delta(|s|) ds &= 2 \int_0^x s^2 \gamma_\delta(|s|) \int_0^1 dt ds + 2 \int_x^\infty s^2 \gamma_\delta(|s|) \int_0^{\frac{x}{s}} dt ds \\
&= 2 \int_0^x s^2 \gamma_\delta(|s|) ds + 2x \int_x^\infty s \gamma_\delta(|s|) ds.
\end{aligned} \tag{1.11}$$

Therefore,

$$\omega_\delta(x, t) = 2 \int_0^x s^2 \gamma_\delta(|s|) ds + 2x \int_x^\infty s \gamma_\delta(|s|) ds. \tag{1.12}$$

It is obvious from here that the derivative with respect to x of this definition of the weight function is

$$\omega'_\delta(x, t) = 2 \int_x^\infty s \gamma_\delta(|s|) ds. \tag{1.13}$$

□

We have a weight function that plays a crucial role in coupling the nonlocal and local diffusion models. This weight function is designed to take the value of 0 in the nonlocal region, where only the nonlocal diffusion model is active, and 1 in the local region, where the local diffusion model fully governs the behavior. In the transitional region, the value of the weight function is calculated based on the arrangement of the kernels, allowing for a smooth transition between the nonlocal and local models.

Definition 3 (Local, Nonlocal, and Quasi-nonlocal Energies, see [15]).

One-dimensional Local Energy

$$E^L(x, t) = \frac{1}{2} \int_{\Omega_L} \omega_\delta(x, t) |u'(x, t)|^2 dx, \tag{1.14}$$

such that weight function

$$\omega_\delta(x, t) = \int_0^1 dt \int_{|s| < \frac{x}{t}} |s|^2 \gamma(|s|) ds. \quad (1.15)$$

One-dimensional Nonlocal Energy

$$E^{NL}(x, t) = \frac{1}{2} \int_{\Omega_{NL}} \int_{\Omega_{NL}} \gamma_\delta(y - x) (u(y, t) - u(x, t))^2 dx dy \quad (1.16)$$

where $\gamma_\delta(y - x)$ is a symmetric kernel, and the relationship between y and x is called a bond (or the "bond" $y - x$).

One-dimensional Quasi-nonlocal Energy

$$E^{QNL}(x, t) = \frac{1}{2} \iint_{x \leq 0 \cup y \leq 0} \gamma_\delta(|y - x|) (u(y, t) - u(x, t))^2 dy dx + \frac{1}{2} \int_{x < 0} |u'(x, t)|^2 \omega_\delta(x, t) dx \quad (1.17)$$

where the weight function is given by

$$\omega_\delta(x) = \int_0^1 dt \int_{|s| < \frac{x}{t}} |s|^2 \gamma(|s|) ds, \quad (1.18)$$

and the kernel $\gamma_\delta(x)$ is defined as

$$\left\{ \begin{array}{l} \gamma_\delta(|x|) = \frac{1}{\delta^3} \gamma\left(\frac{|x|}{\delta}\right), \quad \gamma \text{ is nonnegative and nonincreasing on } (0, 1), \\ \text{with } \text{supp}(\gamma) \subset [0, 1] \text{ and } \int_{\mathbb{R}} |x|^2 \gamma(|x|) dx = 1. \end{array} \right.$$

The energy space of the quasi-nonlocal coupling operator, as well as the connection between local and nonlocal energies, is derived by taking the first variation of the quasi-nonlocal energy functional. This first variation provides the necessary condition for minimizing the total energy, and its computation leads to the creation of an operator that governs the

system. Specifically, the variation of the energy defines an operator that is used to identify the unique curve of shortest length connecting two points in the energy space. This curve represents the optimal transition between nonlocal and local behaviors, ensuring smoothness and energy consistency across the coupled system. By minimizing the energy, the quasi-nonlocal operator achieves a balance between the influences of the local and nonlocal diffusion models, effectively linking the two in a unified framework.

The variation of the combined local and nonlocal energies leads to the formulation of an operator that models the interaction and combination of nonlocal and local diffusion processes. This operator is referred to as the quasi-nonlocal operator. The quasi-nonlocal operator is defined as follows:

Definition 4 (Quasi-nonlocal operator, see [15]).

$$\mathcal{L}^{qnl}u(x) = \begin{cases} 2 \int_{y \in \mathbb{R}} \gamma_\delta(|y-x|)(u(y,t) - u(x,t))dy, & \text{if } x < 0 \\ 2 \int_{y < 0} \gamma_\delta(|y-x|) \left(u(y,t) - u(x,t) \right) dy + (\omega_\delta(x,t)u'(x,t))', & \text{if } x \in [0, \delta) \\ u_{xx}(x,t), & \text{if } x \geq \delta. \end{cases}$$

By taking the first variation of the total energy, which includes contributions from both the nonlocal and local regions, we derive a unified operator that governs the diffusion behavior across the entire domain, seamlessly bridging the local and nonlocal regimes.

Theorem 5. *The quasi-nonlocal operator is the first variation of the total quasi-nonlocal energy for any test function $v \in C^\infty(\Omega)$ [15].*

$$\mathcal{L}^{qnl}(u) = \lim_{\epsilon \rightarrow 0} \frac{E^{QNL}(u + \epsilon v) - E^{QNL}(u)}{\epsilon}$$

Proof.

$$\begin{aligned}
\mathcal{L}^{qnl}(u) &= \lim_{\epsilon \rightarrow 0} \frac{E^{QNL}(u + \epsilon v) - E^{QNL}(u)}{\epsilon} \\
&= \frac{1}{2} \lim_{\epsilon \rightarrow 0} \frac{\iint \gamma_\delta(|y-x|)(u(y,t) + \epsilon v(y,t) - u(x,t) - \epsilon v(x,t))^2 dy dx + \int \omega_\delta(x,t) |u'(x,t) + \epsilon v'(x,t)|^2 dx}{\epsilon} \\
&\quad - \frac{1}{2} \lim_{\epsilon \rightarrow 0} \frac{\iint \gamma_\delta(|y-x|)(u(y,t) - u(x,t)) dy dx + \int \omega_\delta(x,t) |u'(x,t)|^2 dx}{\epsilon} \\
&= \iint \gamma_\delta(|y-x|)(u(x,t)v(x,t) - u(x,t)v(y,t) - u(y,t)v(x,t) + u(y,t)v(y,t)) dy dx \\
&\quad + \omega_\delta(x,t) u'(x,t) v(x,t) \Big|_0^1 - \int (\omega_\delta(x,t) u'(x,t))' v(x,t) dx \\
&= \iint \gamma_\delta(|y-x|)(2u(x,t)v(x,t) - 2u(y,t)v(x,t)) dy dx - \int (\omega_\delta(x,t) u'(x,t))' v(x,t) dx \\
&= -2 \iint_{x \leq 0 \cup y \leq 0} \gamma_\delta(|y-x|)(u(y,t) - u(x,t))v(x,t) dy dx - \int_{x > 0} (\omega_\delta(x,t) u'(x,t))' v(x,t) dx \tag{1.19}
\end{aligned}$$

with assistance from symmetry, boundary conditions, definition of the weight function, and integration by parts. We can similarly define the operator for the nonlocal and local regions by taking the first variation of their energies. The results are the following

$$\begin{aligned}
\mathcal{L}^{qnl}(u) &= \lim_{\epsilon \rightarrow 0} \frac{E^{NL}(u + \epsilon v) - E^{NL}(u)}{\epsilon} \\
&= -2 \int_{y \in R} \gamma_\delta(|y-x|)(u(y,t) - u(x,t))v(x,t) dy, \tag{1.20}
\end{aligned}$$

and

$$\begin{aligned}
\mathcal{L}^{qnl}(u) &= \lim_{\epsilon \rightarrow 0} \frac{E^L(u + \epsilon v) - E^L(u)}{\epsilon} \\
&= -(\omega_\delta(x,t) u'(x,t))' v(x,t) = -u''(x,t) v(x,t). \tag{1.21}
\end{aligned}$$

From here, the coupling operator is pieced together to describe the complete operator. These sections also must be adjusted so they reflect that in the diffusion process force is negative to the first variation of total energy. It can be concluded that the quasi-nonlocal coupling operator by regions are

- **Nonlocal Region:** $x < 0$

$$\mathcal{L}^{qnl}u(x, t) = 2 \int_{y \in R} \gamma_\delta(|y - x|)(u(y, t) - u(x, t))dy. \quad (1.22)$$

- **Transitional Region:** $0 \leq x < \delta$

$$\mathcal{L}^{qnl}u(x, t) = 2 \int_{y < 0} \gamma_\delta(|y - x|)(u(y, t) - u(x, t))dy + (\omega_\delta(x)u'(x, t))'. \quad (1.23)$$

- **Local Region:** $x \geq \delta$

$$\mathcal{L}^{qnl}u(x, t) = u_{xx}(x, t). \quad (1.24)$$

Grouped together as a piecewise function the quasi-nonlocal coupling operator

$$\mathcal{L}^{qnl}u(x) = \begin{cases} 2 \int_{y \in R} \gamma_\delta(|y - x|)(u(y, t) - u(x, t))dy, & \text{if } x < 0 \\ 2 \int_{y < 0} \gamma_\delta(|y - x|)(u(y, t) - u(x, t))dy + (\omega_\delta(x, t)u'(x, t))', & \text{if } x \in [0, \delta) \\ u_{xx}(x, t), & \text{if } x \in [\delta, 1). \end{cases} \quad \square$$

In Chapter 2, we develop a finite difference scheme specifically designed for the quasi-nonlocal coupling model. This numerical approach enables the accurate and efficient simulation of systems that involve both nonlocal and local diffusion processes. By discretizing the quasi-nonlocal operator using a finite difference method, we can approximate the behavior of the system across the entire domain, including the transitional region between the local and nonlocal areas. The finite difference scheme is carefully constructed to ensure stability, consistency, and convergence, making it a robust tool for solving complex coupled diffusion

problems. This method allows for the practical implementation of the quasi-nonlocal model in computational simulations, providing a foundation for the analysis presented in subsequent chapter.

CHAPTER 2: FINITE DIFFERENCE SCHEME FOR QNL COUPLING

See this chapter in [23].

For the last decade, nonlocal integro-differential type models have been employed to describe physical systems. This is due to their natural ability to model physical phenomena at small scales and their reduced regularity requirements which lead to greater flexibility [4, 20, 5, 42, 11, 13, 14, 16, 17, 19, 21, 24, 25, 27, 32, 33, 37, 43]. These nonlocal models are defined through a length scale parameter δ , the horizon, which measures the extent of nonlocal interaction. An important feature of nonlocal models is that they restore the corresponding classical partial differential equation models as the horizon $\delta \rightarrow 0$ [13, 14].

Nonlocal models that are compatible with the local partial differential equations are often very computationally expensive and require additional attention to the boundary treatments since a layer of volumetric boundary conditions is needed within the physical system. Meanwhile, nonlocal models need less regularity requirements which helps the descriptions near defects and singularities. Consequently, tremendous efforts have been devoted to combining nonlocal and local methods to keep accuracy around the irregularity while retaining efficiency away from the singularity. (See the review paper [12] for the state-of-art.)

In [15], a quasi-nonlocal (QNL) coupling method was proposed to combine the nonlocal and local diffusion operators in a seamless way using the variational approach. The coupled operator is proved to preserve many mathematical and physical properties on the continuous level, including the symmetry of operator, the balance of linear momentum, and the maximum principle. However, it is not clear how to retain these desired properties with proper numerical discretization. We will now propose a new finite difference method which inherits all properties from the continuous case.

We recall that the linear local diffusion model in one-dimensional space can be written as

$$u_t(x, t) = u_{xx}(x, t) + f(x, t). \quad (2.1)$$

The corresponding counterpart in the nonlocal setting is the linear nonlocal diffusion model which reads

$$u_t(x, t) = \int_{-\delta}^{\delta} \gamma_{\delta}(s) \left(u(x + s, t) - u(x, t) \right) ds, \quad (2.2)$$

where $\gamma_{\delta}(s)$ denotes the isotropic nonlocal diffusion kernel satisfying the following assumption with $\gamma_{\delta}(\cdot)$ being a rescaled kernel,

$$\begin{cases} \gamma_{\delta}(|s|) = \frac{1}{\delta^3} \gamma\left(\frac{|s|}{\delta}\right), & \gamma \text{ is nonnegative and nonincreasing on } (0,1), \\ \text{with } \text{supp}(\gamma) \subset [0, 1] \text{ and } \int_{-\delta}^{\delta} |s|^2 \gamma(|s|) ds = 2. \end{cases} \quad (2.3)$$

We will display more details about the coupling and numerical schemes in the following sections.

More precisely, we will organize the process as follows. In the first section we recall the energy-based quasi-nonlocal coupling from [15] to build the coupling operator $\mathcal{L}_{\delta}^{qnl}$ bridging the nonlocal and local diffusion problems and introduce space-time discretizations as well as the new finite difference method (FDM). In the next section, we estimate the consistency errors of the proposed scheme using Taylor expansions. The third section's focus is on proving the discrete maximum principle and hence, the stability of proposed scheme. In the next section, we combine the consistency and stability results to conclude the convergence estimates. Then we mathematically study the Courant-Friedrichs-Lewy (CFL) condition for the space-time discretization. In the final two sections, we test several benchmark examples to confirm our theoretical findings, and concluding results.

2.1 Discretized Quasi-Nonlocal Coupling

Now, we consider the domain to be $\Omega_\delta = [-1 - \delta, 1]$, with the coupling interface of nonlocal and local models at $x^* = 0$; $(-1, 0)$ denotes the nonlocal region with nonlocal boundary layer at $[-1 - \delta, -1]$, transitional region $[0, \delta)$, and $[\delta, 1)$ denotes the local region with local boundary point at $\{1\}$, as illustrated in Figure 2.1.

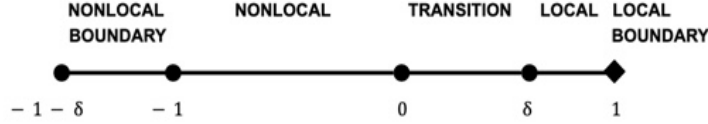


Figure 2.1: Partitioning and boundary layer for a discretized one dimensional domain.

In [15], the quasi-nonlocal operator $\mathcal{L}_\delta^{qnl} u(x, t)$ is introduced to smoothly bridge the local and nonlocal regions over the transitional region $[0, \delta]$. The corresponding coupled diffusion problem is proved to be a well-posed initial value problem and is given by

$$\begin{cases} u_t(x, t) = \mathcal{L}_\delta^{qnl} u(x, t) + f(x, t), & \text{for } T > t > 0 \text{ and } x \in (-1, 1), \\ u(x, 0) = u_0(x), & \text{for } x \in (-1, 1), \\ u(x, t) = 0, & \text{for } x = -1, \text{ or } x = 1. \end{cases} \quad (2.4)$$

\mathcal{L}_δ^{qnl} employed in equation (2.4) is the quasi-nonlocal coupling operator which describes the diffusion within the nonlocal, transitional, and local regions, respectively. The expression of

\mathcal{L}_δ^{qnl} is given below

$$\mathcal{L}_\delta^{qnl}u(x, t) = \begin{cases} \int_{-\delta}^{\delta} \left(u(x+s, t) - u(x, t) \right) \gamma_\delta(s) ds, & \text{if } x \in (-1, 0), \\ \int_x^{\delta} \gamma_\delta(s) \left(u(x-s, t) - u(x, t) \right) ds + \left(\int_x^{\delta} s \gamma_\delta(s) ds \right) u_x(x, t) \\ \quad + \left(\int_0^x s^2 \gamma_\delta(s) + x \int_x^{\delta} s \gamma_\delta(s) ds \right) u_{xx}(x), & \text{if } x \in [0, \delta), \\ u_{xx}(x, t), & \text{if } x \in [\delta, 1). \end{cases} \quad (2.5)$$

Next, we discuss the numerical settings for the spatial and temporal discretization. We use u_i^n to denote the numerical approximation of the exact solution $u(x_i, t^n)$ with spatial and temporal step sizes being with $\Delta x := \frac{1}{N}$ and $\Delta t := \frac{T}{N_T}$, respectively. Hence, the spatial grid is x_i and temporal grid is $t_n = n\Delta t$. For simplicity, we drop x and t but only use i and n accordingly. The relation between Δx and Δt will be determined later by the CFL condition. Meanwhile, we assume that the horizon δ is a multiple of Δx with $\delta = r\Delta x$ and $r \in \mathbb{N}$.

Recall that the entire computational domain is $\Omega_\delta := [-1 - \delta, 1]$, so the interior domain is $\Omega = (-1, 1)$ with interface at $x^* = 0$; the volumetric boundary layer for the nonlocal region is $\Omega_n = [-1 - \delta, -1]$; and the local boundary point is $\Omega_c = \{1\}$. Next we denote the set of spatial grids by I and $I = I_\Omega \cup I_{\Omega_n} \cup I_{\Omega_c}$, where $I_\Omega = \{1, 2, \dots, 2N - 1\}$ denotes the interior grids, $I_{\Omega_n} = \{-(r-1), \dots, 0\}$ denotes the nonlocal volumetric boundary grids, and $I_{\Omega_c} = \{2N\}$ denotes the local boundary point.

Following the scope of asymptotically compatible schemes [45, 46], we define the spatial discretization of the quasi-nonlocal coupling operator $\mathcal{L}_{\delta, \Delta x}^{qnl}$ as follows.

Definition 5. *Discretized Quasi-nonlocal Coupling Operator*

$$\mathcal{L}_{\delta, \Delta x}^{qnl} u_i^n = \begin{cases} \sum_{j=1}^r \frac{u_{i+j}^n - 2u_i^n + u_{i-j}^n}{(j\Delta x)^2} \int_{(j-1)\Delta x}^{j\Delta x} s^2 \gamma_\delta(s) ds, & \text{if } x_i < 0, \\ \sum_{j=\frac{x_i}{\Delta x}+1}^r \frac{u_{i+j-1}^n - 2u_i^n + u_{i-j+1}^n}{2(j-1)\Delta x} \int_{(j-1)\Delta x}^{j\Delta x} s \gamma_\delta(s) ds \\ - \sum_{j=\frac{x_i}{\Delta x}+1}^r \frac{u_{i+j-1}^n - u_{i-j+1}^n}{2(j-1)\Delta x} \int_{(j-1)\Delta x}^{j\Delta x} s \gamma_\delta(s) ds \\ + \left(\int_{x_i}^{\delta} s \gamma_\delta(s) ds \right) \frac{u_{i+1}^n - u_i^n}{\Delta x} \\ + \left(\int_0^{x_i} s^2 \gamma_\delta(s) ds + x_i \int_{x_i}^{\delta} s \gamma_\delta(s) ds \right) \frac{u_{i+1}^n - 2u_i^n + u_{i-1}^n}{(\Delta x)^2}, & \text{if } x_i \in [0, \delta), \\ \frac{u_{i+1}^n - 2u_i^n + u_{i-1}^n}{(\Delta x)^2}, & \text{if } x_i \in [\delta, 1). \end{cases} \quad (2.6)$$

For the temporal discretization, we employ the simplest explicit Euler scheme due to the limitation of first order accuracy in the spatial discretization, which will be proved later. Hence the full finite difference method discretization of (2.4) is

$$\frac{u_i^{n+1} - u_i^n}{\Delta t} = \mathcal{L}_{\delta, \Delta x}^{qnl} u_i^n + f_i^n, \quad i \in I_\Omega, \quad (2.7)$$

where $f_i^n = f(x_i, t^n)$.

Figure 2.2 displays a sampling set of spatial stencils using $N = 5$ on domain $[-1 - \delta, 1]$. The step size is $\Delta x = \frac{1}{5}$ and the horizon $\delta = r\Delta x$ with $r = 3$.

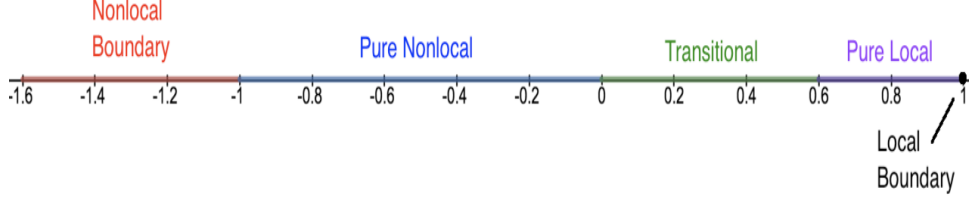


Figure 2.2: Example finite difference stencil with $\Delta x = \frac{1}{5}$, horizon $\delta = r\Delta x$, and $r = 3$.

Remark 1. In [15], the time-integral is still approximated by the explicit Euler method, and the $\tilde{\mathcal{L}}_{\delta, \Delta x}^{qnl}$ is approximated by the following finite difference scheme given the interface at $x^* = 0$:

$$\tilde{\mathcal{L}}_{\delta, \Delta x}^{qnl} u_i^n \approx \begin{cases} 2 \sum_{j=1}^r \frac{u_{i+j}^n - 2u_i^n + u_{i-j}^n}{(j\Delta x)^2} \int_{(j-1)\Delta x}^{j\Delta x} s^2 \gamma_\delta(s) ds, & \text{if } x_i < 0. \\ \sum_{j=\frac{x_i}{\Delta x}}^r \frac{u_{i+j}^n - 2u_i^n + u_{i-j}^n}{(j\Delta x)^2} \int_{(j-1)\Delta x}^{j\Delta x} s^2 \gamma_\delta(s) ds \\ - \sum_{j=\frac{x_i}{\Delta x}}^r \frac{u_{i+j}^n - u_{i-j}^n}{j\Delta x} \int_{(j-1)\Delta x}^{j\Delta x} s \gamma_\delta(s) ds \\ + 2 \left(\int_{x_i}^{\delta} s \gamma_\delta(s) ds \right) \frac{u_{i+1}^n - u_i^n}{\Delta x} \\ + \left(2 \int_0^{x_i} s^2 \gamma_\delta(s) ds + 2x_i \int_{x_i}^{\delta} s \gamma_\delta(s) ds \right) \frac{u_{i+1}^n - 2u_i^n + u_{i-1}^n}{(\Delta x)^2}, & \text{if } x_i \in [0, \delta), \\ \frac{u_{i+1}^n - 2u_i^n + u_{i-1}^n}{(\Delta x)^2}, & \text{if } x_i \in [\delta, 1). \end{cases} \quad (2.8)$$

Comparing (2.6) with (2.8), we notice that the difference is replacing j in the original scheme by $(j - 1)$ in the new scheme. This is the main difference in the approximation that allows the equation (2.6) to satisfy the discrete maximum principle whereas equation (2.8) does not. We will rigorously prove this in Section 2.3.

Remark 2. For numerical schemes that preserve the maximum principles in high dimensional space there are other types of coupling methods developed for two-dimensional problems. [47, 50] These coupling schemes are based on a domain-decomposition methods via Neumann or Robin type boundary conditions, and are rigorously proved to keep the maximum principles.

Regarding the conservation of flux, notice that the operator $\mathcal{L}_{\delta, \Delta x}^{qnl}$ of new scheme (2.6) is symmetric, hence, it possesses this property. In general, one has to keep interaction symmetries across the transitional region of the coupling region. However, the nonlocal neighborhood, $B_\delta(x)$, becomes a disk (in two dimensions) or a ball (in three dimensions), making the intersections with the interface more complex. As a result, it is not easy to preserve the flux in higher dimensions.

2.2 Consistency of the Discretized Quasi-Nonlocal Operator

In this section, we estimate the consistency error of the scheme (2.7) with $\mathcal{L}_{\delta, \Delta x}^{qnl}$ defined in (2.6).

Theorem 6. Let the horizon $\delta = r\Delta x$ with $r \in \mathbb{N}$ being fixed, and suppose $u(x, t)$ is the strong solution to (2.4), and u_i^n is the discrete solution to the scheme (2.7) with $i \in I_\Omega$ and $t^n = n\Delta t$. Also assume that the exact solution u is sufficiently smooth, specifically $u(x, t) \in C^4([-1-\delta, 1] \times [0, T])$. Suppose at any given time level $t^n = n\Delta t$ we have $u(x_i, t^n) = u_i^n$, for all $i \in I_\Omega = \{1, \dots, 2N - 1\}$, then for the next time level $n + 1$ the consistency error of the scheme satisfies

$$|u_i^{n+1} - u(x_i, t^{n+1})| \leq C_\delta \Delta t ((\Delta x) + (\Delta t)), \text{ for all } i = 1, \dots, 2N - 1, \quad (2.9)$$

where C_δ is a constant independent of Δx and Δt .

Proof. We evolve $u(x_i, t^n)$ and u_i^n by one time step Δt according to three differential regions.

Local: If $x_i > \delta$ or simply $i \in \{N + r + 1, \dots, 2N - 1\}$, then the continuous and discrete

equations follow the expressions in the local region. So at (x_i, t^n) , we have the continuous equation:

$$u_t(x_i, t^n) = u_{xx}(x_i, t^n) + f(x_i, t^n), \quad (2.10)$$

and the discrete equation:

$$\frac{u_i^{n+1} - u_i^n}{\Delta t} = \frac{u_{i+1}^n - 2u_i^n + u_{i-1}^n}{(\Delta x)^2} + f_i^n \quad (2.11)$$

with $f_i^n = f(x_i, t^n)$.

Notice from the consistency assumption that $u_i^n = u(x_i, t^n)$, so we can rewrite the discrete equation as

$$\frac{u_i^{n+1} - u(x_i, t^n)}{\Delta t} = \frac{u(x_{i+1}, t^n) - 2u(x_i, t^n) + u(x_{i-1}, t^n)}{(\Delta x)^2} + f(x_i, t^n). \quad (2.12)$$

We apply the Taylor expansion at the spatial grid (x_i) up to the fourth-order derivative and obtain an estimate of u_i^{n+1} , which is

$$\begin{aligned} u_i^{n+1} &= u(x_i, t^n) + \Delta t \left(\frac{u(x_{i+1}, t^n) - 2u(x_i, t^n) + u(x_{i-1}, t^n)}{(\Delta x)^2} + f(x_i, t^n) \right) \\ &= u(x_i, t^n) + \Delta t \left(\frac{(\Delta x)^2 u_{xx}(x_i, t^n) + O(\Delta x^4)}{(\Delta x)^2} + f(x_i, t^n) \right) \\ &= u(x_i, t^n) + \Delta t \left(u_{xx}(x_i, t^n) + f(x_i, t^n) \right) + O(\Delta t (\Delta x)^2). \end{aligned} \quad (2.13)$$

Now, let us estimate the continuous solution $u(x_i, t^{n+1})$. This time, we apply the Taylor expansion at the time grid (t^n) and get

$$\begin{aligned} u(x_i, t^{n+1}) &= u(x_i, t^n) + \Delta t u_t(x_i, t^n) + O(\Delta t^2) \\ &= u(x_i, t^n) + \Delta t \left[(u_{xx}(x_i, t^n) + f(x_i, t^n)) \right] + O(\Delta t^2), \end{aligned} \quad (2.14)$$

where we substitute $u_t(x_i, t^n)$ by the continuous equation on the local region.

By subtracting (2.13) from (2.14) we obtain

$$u_i^{n+1} - u(x_i, t^{n+1}) = O(\Delta t(\Delta x)^2) + O((\Delta t)^2). \quad (2.15)$$

Nonlocal: Next we consider the fully nonlocal region where $x_i \leq 0$ or simply $i \in \{1, \dots, N\}$.

We first have the continuous equation:

$$\begin{aligned} u_t(x_i, t^n) &= \int_{-\delta}^{\delta} \gamma_{\delta}(s) \left(u(x_i + s, t^n) - u(x_i, t^n) \right) ds + f(x_i, t^n) \\ &= \int_{-\delta}^0 \gamma_{\delta}(s) \left(u(x_i + s, t^n) - u(x_i, t^n) \right) ds \\ &\quad + \int_0^{\delta} \gamma_{\delta}(s) \left(u(x_i + s, t^n) - u(x_i, t^n) \right) ds + f(x_i, t^n) \\ &= \int_0^{\delta} \gamma_{\delta}(-s) \left(u(x_i - s, t^n) - u(x_i, t^n) \right) ds \\ &\quad + \int_0^{\delta} \gamma_{\delta}(s) \left(u(x_i + s, t^n) - u(x_i, t^n) \right) ds + f(x_i, t^n). \end{aligned} \quad (2.16)$$

Because of the isotropic property of the nonlocal kernel $\gamma_{\delta}(s)$ summarized in (2.3), we have

$$u_t(x_i, t^n) = \int_0^{\delta} \gamma_{\delta}(s) \left(u(x_i + s, t^n) - 2u(x_i, t^n) + u(x_i - s, t^n) \right) ds + f(x_i, t^n). \quad (2.17)$$

Clearly, we can divide the integral into the sum of subintegrals on the union of subintervals, so we have,

$$u_t(x_i, t^n) = \sum_{j=1}^r \int_{(j-1)\Delta x}^{j\Delta x} \gamma_{\delta}(s) \left(u(x_i + s, t^n) - 2u(x_i, t^n) + u(x_i - s, t^n) \right) ds + f(x_i, t^n). \quad (2.18)$$

Meanwhile, we have the discrete equation to advance u_i^n to u_i^{n+1} :

$$\frac{u_i^{n+1} - u_i^n}{\Delta t} = \sum_{j=1}^r \frac{u_{i+j}^n - 2u_i^n + u_{i-j}^n}{(j\Delta x)^2} \int_{(j-1)\Delta x}^{j\Delta x} s^2 \gamma_{\delta}(s) ds + f_i^n. \quad (2.19)$$

This gives,

$$u_i^{n+1} = u_i^n + \Delta t \left(\sum_{j=1}^r \frac{u_{i+j}^n - 2u_i^n + u_{i-j}^n}{(j\Delta x)^2} \int_{(j-1)\Delta x}^{j\Delta x} s^2 \gamma_\delta(s) ds + f_i^n \right). \quad (2.20)$$

Now we want to estimate the continuous solution $u(x_i, t^{n+1})$. We know that

$$u(x_i, t^{n+1}) = u(x_i, t^n) + \Delta t u_t(x_i, t^n) + O(\Delta t^2). \quad (2.21)$$

Hence, inserting the continuous description of the nonlocal diffusion, (2.18), we obtain

$$\begin{aligned} u(x_i, t^{n+1}) &= u(x_i, t^n) + \Delta t u_t(x_i, t^n) + O(\Delta t^2) \\ &= u(x_i, t^n) + \Delta t \left[\sum_{j=1}^r \int_{(j-1)\Delta x}^{j\Delta x} \gamma_\delta(s) s^2 \left(\frac{u(x_i + s, t^n) - 2u(x_i, t^n) + u(x_i - s, t^n)}{s^2} \right) ds \right. \\ &\quad \left. + f(x_i, t^n) \right] + O(\Delta t^2) \end{aligned} \quad (2.22)$$

for each integral term from $[(j-1)\Delta x, j\Delta x]$ within the summation. We then focus on the fractional term and apply a Taylor expansion to $u(x_i + s, t^n)$ and $u(x_i - s, t^n)$ for s at $(j\Delta x)$ up to a fourth-order derivative. This gives an estimate of

$$\begin{aligned} u(x_i, t^{n+1}) &= u(x_i, t^n) \\ &\quad + \Delta t \left[\sum_{j=1}^r \int_{(j-1)\Delta x}^{j\Delta x} \gamma_\delta(s) s^2 \frac{1}{(j\Delta x)^2} \left((u(x_{i+j}, t^n) - 2u(x_i, t^n) + u(x_{i-j}, t^n)) + O(s^4) \right) ds \right. \\ &\quad \left. + f(x_i, t^n) \right] + O(\Delta t^2) \\ &= u_i^n + \Delta t \left[\sum_{j=1}^r \int_{(j-1)\Delta x}^{j\Delta x} \gamma_\delta(s) s^2 \frac{1}{(j\Delta x)^2} \left((u_{i+j}^n - 2u_i^n + u_{i-j}^n) \right) ds + O(\Delta x^2) \right. \\ &\quad \left. + f(x_i, t^n) \right] + O(\Delta t^2). \end{aligned} \quad (2.23)$$

Then by subtracting (2.20) from (2.23), we can get

$$u_i^{n+1} - u(x_i, t^{n+1}) = O(\Delta t) \cdot O(\Delta x)^2 + O(\Delta t^2). \quad (2.24)$$

Transitional: Finally we consider when $x_i \in (0, \delta]$ or equivalently $i \in \{N + 1, \dots, N + r\}$, and again we will look at the continuous equation for the time derivative $u_t(x_i, t^n)$ first.

$$\begin{aligned} u_t(x_i, t^n) = & \left[\int_{x_i}^{\delta} \gamma_{\delta}(s) \left(u(x_i - s, t^n) - u(x_i, t^n) \right) ds + \left(\int_{x_i}^{\delta} s \gamma_{\delta}(s) ds \right) u_x(x_i, t^n) \right. \\ & \left. + \left(\int_0^{x_i} s^2 \gamma_{\delta}(s) ds + x_i \int_{x_i}^{\delta} s \gamma_{\delta}(s) ds \right) u_{xx}(x_i, t^n) \right] + f(x_i, t^n), \end{aligned} \quad (2.25)$$

and splitting symmetrically the first integral gives

$$\begin{aligned} u_t(x_i, t^n) = & \int_{x_i}^{\delta} \frac{\gamma_{\delta}(s)}{2} \left(u(x_i - s, t^n) - 2u(x_i, t^n) + u(x_i + s, t^n) \right) ds \\ & + \int_{x_i}^{\delta} \frac{\gamma_{\delta}(s)}{2} \left(u(x_i - s, t^n) - u(x_i + s, t^n) \right) ds + \left(\int_{x_i}^{\delta} s \gamma_{\delta}(s) ds \right) u_x(x_i, t^n) \\ & + \left(\int_0^{x_i} s^2 \gamma_{\delta}(s) ds + x_i \int_{x_i}^{\delta} s \gamma_{\delta}(s) ds \right) u_{xx}(x_i, t^n) + f(x_i, t^n), \end{aligned} \quad (2.26)$$

and dividing these two integrals into the sum of subintegrals on the union of subintervals, and modifying each integrand in the scope of the asymptotically compatible scheme [46], we find

$$\begin{aligned} u_t(x_i, t^n) = & \sum_{j=\frac{x_i}{\Delta x}+1}^r \int_{(j-1)\Delta x}^{j\Delta x} \frac{\gamma_{\delta}(s)s}{2} \left(\frac{u(x_i - s, t^n) - 2u(x_i, t^n) + u(x_i + s, t^n)}{s} \right) ds \\ & + \sum_{j=\frac{x_i}{\Delta x}+1}^r \int_{(j-1)\Delta x}^{j\Delta x} \frac{\gamma_{\delta}(s)s}{2} \left(\frac{u(x_i - s, t^n) - u(x_i + s, t^n)}{s} \right) ds + \left(\int_{x_i}^{\delta} s \gamma_{\delta}(s) ds \right) u_x(x_i, t^n) \\ & + \left(\int_0^{x_i} s^2 \gamma_{\delta}(s) ds + x_i \int_{x_i}^{\delta} s \gamma_{\delta}(s) ds \right) u_{xx}(x_i, t^n) + f(x_i, t^n). \end{aligned} \quad (2.27)$$

Now working with the discrete equation for u_i^{n+1}

$$\begin{aligned}
\frac{u_i^{n+1} - u_i^n}{\Delta t} &= \sum_{j=\frac{x_i}{\Delta x}+1}^r \frac{u_{i+j-1}^n - 2u_i^n + u_{i-j+1}^n}{2(j-1)\Delta x} \int_{(j-1)\Delta x}^{j\Delta x} s\gamma_\delta(s)ds \\
&- \sum_{j=\frac{x_i}{\Delta x}+1}^r \frac{u_{i+j-1}^n - u_{i-j+1}^n}{2(j-1)\Delta x} \int_{(j-1)\Delta x}^{j\Delta x} s\gamma_\delta(s)ds + \left(\int_{x_i}^{\delta} s\gamma_\delta(s)ds \right) \frac{u_{i+1}^n - u_i^n}{\Delta x} \\
&+ \left(\int_0^{x_i} s^2\gamma_\delta(s)ds + x_i \int_{x_i}^{\delta} s\gamma_\delta(s)ds \right) \frac{u_{i+1}^n - 2u_i^n + u_{i-1}^n}{(\Delta x)^2} + f_i^n. \tag{2.28}
\end{aligned}$$

This gives,

$$\begin{aligned}
u_i^{n+1} &= u_i^n + \Delta t \left[\sum_{j=\frac{x_i}{\Delta x}+1}^r \frac{u_{i+j-1}^n - 2u_i^n + u_{i-j+1}^n}{2(j-1)\Delta x} \int_{(j-1)\Delta x}^{j\Delta x} s\gamma_\delta(s)ds \right. \\
&- \sum_{j=\frac{x_i}{\Delta x}+1}^r \frac{u_{i+j-1}^n - u_{i-j+1}^n}{2(j-1)\Delta x} \int_{(j-1)\Delta x}^{j\Delta x} s\gamma_\delta(s)ds + \left(\int_{x_i}^{\delta} s\gamma_\delta(s)ds \right) \frac{u_{i+1}^n - u_i^n}{\Delta x} \\
&\left. + \left(\int_0^{x_i} s^2\gamma_\delta(s)ds + x_i \int_{x_i}^{\delta} s\gamma_\delta(s)ds \right) \frac{u_{i+1}^n - 2u_i^n + u_{i-1}^n}{(\Delta x)^2} + f_i^n \right]. \tag{2.29}
\end{aligned}$$

Again we want to estimate difference between $u(x_i, t^{n+1})$ and u_i^{n+1} .

For each integral term $[(j-1)\Delta x, j\Delta x]$ within the summation of (2.27), we then use a Taylor expansion for $u(x_i + s, t^n)$ and $u(x_i - s, t^n)$ for s at $(j-1)\Delta x$, which is similar to the processing we did for the nonlocal region.

$$\begin{aligned}
u(x_i, t^{n+1}) &= u(x_i, t^n) \\
&+ \Delta t \left[\sum_{j=\frac{x_i}{\Delta x}+1}^r \int_{(j-1)\Delta x}^{j\Delta x} \frac{\gamma_\delta(s)s}{2(j-1)\Delta x} \left(u(x_{i+j-1}, t^n) - 2u(x_i, t^n) + u(x_{i-j+1}, t^n) + O(s^2) \right) ds \right. \\
&+ \sum_{j=\frac{x_i}{\Delta x}+1}^r \int_{(j-1)\Delta x}^{j\Delta x} \frac{\gamma_\delta(s)s}{2(j-1)\Delta x} \left(u(x_{i+j-1}, t^n) - u(x_{i-j+1}, t^n) + O(s) \right) ds \\
&+ \left(\int_{x_i}^{\delta} s \gamma_\delta(s) ds \right) \left(\frac{u(x_{i+1}, t^n) - u(x_i, t^n)}{\Delta x} + O(\Delta x) \right) \\
&+ \left(\int_0^{x_i} s^2 \gamma_\delta(s) ds + x_i \int_{x_i}^{\delta} s \gamma_\delta(s) ds \right) \left(\frac{u(x_{i+1}, t^n) - 2u(x_i, t^n) + u(x_{i-1}, t^n)}{\Delta x^2} + O(\Delta x^2) \right) \\
&\left. + f(x_i, t^n) \right] + O(\Delta t^2). \tag{2.30}
\end{aligned}$$

By subtracting (2.29) from (2.30) we have

$$u_i^{n+1} - u(x_i, t^{n+1}) = O(\Delta t)O(\Delta x) + O(\Delta t^2). \tag{2.31}$$

Therefore, $\|u(x_i, t^{n+1}) - u_i^{n+1}\|_{L^\infty} = O(\Delta t)O(\Delta x) + O(\Delta t^2)$ with the highest restrictions from the transitional region. Since the order of accuracy is greater than zero, the finite difference scheme is consistent. \square

2.3 Stability of the Discretized Quasi-nonlocal Operator

Global stability of the scheme is attained by the discrete maximum principle. To prove the discrete maximum principle for the quasi-nonlocal coupling equation with an underlying finite difference discretization the spatial operator $(-\mathcal{L}_{\delta, \Delta x}^{qnl})$ must be positive-definite, and the time discretization, that is a single explicit Euler integrator, must be a convex scheme. Recall the domain $\Omega = [-1, 1]$ with interface at $x^* = 0$. The volumetric boundary layer for the nonlocal region is $\Omega_n = (-1 - \delta, -1]$, and the local boundary point is $\Omega_c = \{1\}$. The corresponding sets of spatial grids are $I_\Omega = \{1, 2, \dots, 2N - 1\}$ for Ω , $I_{\Omega_n} = \{-(r - 1), \dots, 0\}$

for Ω_n , and $I_{\Omega_c} = \{2N\}$ for Ω_c . Let $I = I_\Omega \cup I_{\Omega_n} \cup I_{\Omega_c}$ denote the union of total stencils within the entire domain (Interior and Boundary), and $I_B = I_{\Omega_n} \cup I_{\Omega_c}$ denote the stencils within the boundary regions $\Omega_n \cup \Omega_c$ (Boundary).

Next we will prove the positive-definiteness of $(-\mathcal{L}_{\delta, \Delta x}^{qnl})$ in Theorem 7, which is the discrete maximum principle for the static case; and then extend the result to the dynamic case in Theorem 8 where the time derivative is involved.

Theorem 7. Discrete Maximum Principle for the Static Case *The discrete operator $\mathcal{L}_{\delta, \Delta x}^{qnl}$ satisfies the maximum principle. For $u(x_i) \in \ell^1(I)$ with $(-\mathcal{L}_{\delta, \Delta x}^{qnl})(u(x_j)) \leq 0$ and $j \in I_\Omega$, and for any $i \in I = I_\Omega \cup I_B$, we have*

$$\max_{i \in I} u(x_i) \leq \max_{i \in I_B} u(x_i). \quad (2.32)$$

Furthermore, equality holds, and $u(x_i)$ is a constant function on stencils I .

Proof. Suppose the discrete function u achieves its strictly maximum values at an interior grid $j^* \in I_\Omega$.

Case I Nonlocal: Consider $j^* \in \{1, 2, \dots, N\}$. Then since $u(x_{j^*})$ is a strict maximum

$$\mathcal{L}_{\delta, \Delta x}^{qnl} u_h(x_{j^*}) = \sum_{k=1}^r \frac{u(x_{j^*+k}) - 2u(x_{j^*}) + u(x_{j^*-k}))}{(k\Delta x)^2} \int_{(k-1)\Delta x}^{k\Delta x} s^2 \gamma_\delta(s) ds < 0 \quad (2.33)$$

which contradicts $-\mathcal{L}_{\delta, \Delta x}^{qnl} u(x_{j^*}) \leq 0$ unless u is constant.

Case II Transitional: Consider $j^* \in \{N+1, N+2, \dots, N+r\}$. We observe that

$$\int_{(k-1)\Delta x}^{k\Delta x} s^2 \gamma_\delta(s) ds > (k-1)\Delta x \int_{(k-1)\Delta x}^{k\Delta x} s \gamma_\delta(s) ds. \quad (2.34)$$

Using $u(x_{j^*})$

$$\begin{aligned}
\mathcal{L}_{\delta, \Delta x}^{qnl} u_h(x_{j^*}) &= \sum_{k=\frac{x_{j^*}}{\Delta x}+1}^r \frac{u(x_{j^*+k-1}) - 2u(x_{j^*}) + u(x_{j^*-k+1}))}{2(k-1)^2(\Delta x)^2} \int_{(k-1)\Delta x}^{k\Delta x} s^2 \gamma_\delta(s) ds \\
&- \sum_{k=\frac{x_{j^*}}{\Delta x}+1}^r \frac{u(x_{j^*+k-1}) - u(x_{j^*-k+1}))}{2(k-1)\Delta x} \int_{(k-1)\Delta x}^{k\Delta x} s \gamma_\delta(s) ds \\
&+ \left(\int_{x_{j^*}}^{\delta} s \gamma_\delta(s) ds \right) \frac{u(x_{j^*+1}) - u(x_{j^*})}{\Delta x} \\
&+ \left(\int_0^{x_{j^*}} s^2 \gamma_\delta(s) ds + x_{j^*} \int_{x_{j^*}}^{\delta} s \gamma_\delta(s) ds \right) \frac{u(x_{j^*+1}) - 2u(x_{j^*}) + u(x_{j^*-1}))}{(\Delta x)^2}. \quad (2.35)
\end{aligned}$$

Also since $u(x_{j^*})$ is a strict maximum we know

$$\frac{u(x_{j^*+k-1}) - 2u(x_{j^*}) + u(x_{j^*-k+1}))}{2(k-1)^2(\Delta x)^2} < 0, \quad (2.36)$$

and combined with (2.34), this gives

$$\begin{aligned}
\mathcal{L}_{\delta, \Delta x}^{qnl} u(x_{j^*}) &\leq \sum_{k=\frac{x_{j^*}}{\Delta x}+1}^r \frac{u(x_{j^*+k-1}) - 2u(x_{j^*}) + u(x_{j^*-k+1}))}{2(k-1)^2(\Delta x)^2} \cdot (k-1)\Delta x \int_{(k-1)\Delta x}^{k\Delta x} s \gamma_\delta(s) ds \\
&- \sum_{k=\frac{x_{j^*}}{\Delta x}+1}^r \frac{u(x_{j^*+k-1}) - u(x_{j^*-k+1}))}{2(k-1)\Delta x} \int_{(k-1)\Delta x}^{k\Delta x} s \gamma_\delta(s) ds \\
&+ \left(\int_{x_{j^*}}^{\delta} s \gamma_\delta(s) ds \right) \frac{u(x_{j^*+1}) - u(x_{j^*})}{\Delta x} \\
&+ \left(\int_0^{x_{j^*}} s^2 \gamma_\delta(s) ds + x_{j^*} \int_{x_{j^*}}^{\delta} s \gamma_\delta(s) ds \right) \frac{u(x_{j^*+1}) - 2u(x_{j^*}) + u(x_{j^*-1}))}{(\Delta x)^2}. \quad (2.37)
\end{aligned}$$

Simplifying we conclude

$$\begin{aligned}
\mathcal{L}_{\delta, \Delta x}^{qnl} u_h(x_{j^*}) &\leq \sum_{k=\frac{x_{j^*}}{\Delta x}+1}^r \frac{-2u(x_{j^*}) + 2u(x_{j^*-k+1})}{2(k-1)\Delta x} \int_{(k-1)\Delta x}^{k\Delta x} s\gamma_\delta(s)ds \\
&+ \left(\int_{x_{j^*}}^{\delta} s\gamma_\delta(s)ds \right) \frac{u(x_{j^*+1}) - u(x_{j^*})}{\Delta x} \\
&+ \left(\int_0^{x_{j^*}^*} s^2\gamma_\delta(s)ds + x_{j^*} \int_{x_{j^*}}^{\delta} s\gamma_\delta(s)ds \right) \frac{u(x_{j^*+1}) - 2u(x_{j^*}) + u(x_{j^*-1})}{(\Delta x)^2} < 0.
\end{aligned} \tag{2.38}$$

which contradicts $-\mathcal{L}_{\delta, \Delta x}^{qnl} u(x_j) \leq 0$.

Case III Local: Consider $j^* \in \{N + r + 1, \dots, 2N - 1\}$. Then since $u(x_{j^*})$ is a strict maximum

$$\mathcal{L}_{\delta, \Delta x}^{qnl} u(x_{j^*}) = \frac{u(x_{j^*+1}) - 2u(x_{j^*}) + u(x_{j^*-1})}{(\Delta x)^2} < 0 \tag{2.39}$$

which contradicts $-\mathcal{L}_{\delta, \Delta x}^{qnl} u(x_j) \leq 0$. □

Next, we will consider the time-dependent case.

Theorem 8. Discrete Maximum Principle for the dynamic case Suppose for $i \in I = I_\Omega \cup I_B$ and $n = 0, 1, \dots, N_T - 1$ with $T = N_T \cdot \Delta t$ that $\{u_i^n\}$ solves the following discrete quasi-nonlocal diffusion equation.

$$\begin{cases} \frac{u_i^{n+1} - u_i^n}{\Delta t} = \mathcal{L}_{\delta, \Delta x}^{qnl} u_i^n + f_i^n, & \text{for } i \in I_\Omega, \text{ and } N_T > n \geq 0, \\ u_i^0 = g_i^0, & \text{for } i \in I \text{ (Initial Condition),} \\ u_i^n = q_i^n, & \text{for } i \in I_B, n \geq 0 \text{ (Boundary Condition),} \end{cases} \tag{2.40}$$

then u_i^n satisfies the discrete maximum principle

$$u_i^n \leq \max\{g_i^0 |_{i \in I}, q_i^n |_{i \in I_B, n \geq 0}\} \tag{2.41}$$

given that $f_i^n \leq 0$ for all $i \in I_\Omega$, all $n \geq 0$, and $\frac{\Delta t}{\Delta x^2} \leq \frac{1}{4}$.

Proof. We denote $M = \max\{g_i^0|_{i \in I}, q_i^n|_{i \in I_B, n \geq 0}\}$. Clearly, at $n = 0$ we have $u_i^0 \leq M$ for all $i \in I = I_\Omega \cup I_B$. We assume that this holds for $n = m$ with $0 \leq m \leq N_T - 2$. Now we would like to advance it to the next time level $n = m + 1$.

Case I Nonlocal: Consider $i \in \{1, 2, \dots, N\}$ which is the nonlocal region. Then

$$\begin{aligned} u_i^{m+1} &= u_i^m + \Delta t \left(\mathcal{L}_{\delta, \Delta x}^{qnl} u_i^m + f_i^m \right) \\ &\leq u_i^m + \Delta t \mathcal{L}_{\delta, \Delta x}^{qnl} u_i^m \\ &= \left(1 - \frac{2\Delta t}{\Delta x^2} \sum_{k=1}^r \frac{1}{k^2} \int_{(k-1)\Delta x}^{k\Delta x} s^2 \gamma_\delta(s) ds \right) u_i^m + \frac{\Delta t}{\Delta x^2} \sum_{k=1}^r \frac{u_{i+k}^m + u_{i-k}^m}{k^2} \int_{(k-1)\Delta x}^{k\Delta x} s^2 \gamma_\delta(s) ds. \end{aligned}$$

Notice that

$$\sum_{k=1}^r \frac{1}{k^2} \int_{(k-1)\Delta x}^{k\Delta x} s^2 \gamma_\delta(s) ds \leq \sum_{k=1}^r \int_{(k-1)\Delta x}^{k\Delta x} s^2 \gamma_\delta(s) ds = \int_0^\delta s^2 \gamma_\delta(s) ds = 1 \quad (2.42)$$

and $\frac{\Delta t}{\Delta x^2} \leq \frac{1}{4}$, so

$$\left(1 - \frac{2\Delta t}{\Delta x^2} \sum_{k=1}^r \frac{1}{k^2} \int_{(k-1)\Delta x}^{k\Delta x} s^2 \gamma_\delta(s) ds \right) \geq 0. \quad (2.43)$$

Hence,

$$\begin{aligned} u_i^{m+1} &\leq \left(1 - \frac{2\Delta t}{\Delta x^2} \sum_{k=1}^r \frac{1}{k^2} \int_{(k-1)\Delta x}^{k\Delta x} s^2 \gamma_\delta(s) ds \right) u_i^m + \frac{\Delta t}{\Delta x^2} \sum_{k=1}^r \frac{u_{i+k}^m + u_{i-k}^m}{k^2} \int_{(k-1)\Delta x}^{k\Delta x} s^2 \gamma_\delta(s) ds \\ &\leq \left(1 - \frac{2\Delta t}{\Delta x^2} \sum_{k=1}^r \frac{1}{k^2} \int_{(k-1)\Delta x}^{k\Delta x} s^2 \gamma_\delta(s) ds \right) M + \frac{\Delta t}{\Delta x^2} \sum_{k=1}^r \frac{M + M}{k^2} \int_{(k-1)\Delta x}^{k\Delta x} s^2 \gamma_\delta(s) ds \\ &= M. \end{aligned} \quad (2.44)$$

Case II Transitional: Consider $i \in \{N + 1, \dots, N + r\}$ which is the transitional region.

Then

$$\begin{aligned}
u_i^{m+1} &\leq u_i^m + \Delta t \mathcal{L}_{\delta, \Delta x}^{qnl} u_i^m \\
&= u_i^m + \Delta t \left[\sum_{k=\frac{x_i}{\Delta x}+1}^r \frac{u_{i+k-1}^m - 2u_i^m + u_{i-k+1}^m}{2(k-1)^2 \Delta x^2} \int_{(k-1)\Delta x}^{k\Delta x} s^2 \gamma_\delta(s) ds \right. \\
&\quad - \sum_{k=\frac{x_i}{\Delta x}+1}^r \frac{u_{i+k-1}^m - u_{i-k+1}^m}{2(k-1)\Delta x} \int_{(k-1)\Delta x}^{k\Delta x} s \gamma_\delta(s) ds + \left(\int_{x_i}^\delta s \gamma_\delta(s) ds \right) \frac{u_{i+1}^m - u_i^m}{\Delta x} \\
&\quad \left. + \left(\int_0^{x_i} s^2 \gamma_\delta(s) ds + x_i \int_{x_i}^\delta s \gamma_\delta(s) ds \right) \frac{u_{i+1}^m - 2u_i^m + u_{i-1}^m}{\Delta x^2} \right] \\
&= A \cdot u_i^m + \sum_{k=\frac{x_i}{\Delta x}+1}^r (B_k \cdot u_{i+k-1}^m + C_k \cdot u_{i-k+1}^m + D \cdot u_{i+1}^m + E \cdot u_{i-1}^m) \tag{2.45}
\end{aligned}$$

where those notations are defined as

$$\begin{aligned}
A &= 1 + \frac{\Delta t}{\Delta x^2} \left(\sum_{k=\frac{x_i}{\Delta x}+1}^r \frac{-1}{(k-1)^2} \int_{(k-1)\Delta x}^{k\Delta x} s^2 \gamma_\delta(s) ds \right) + \frac{\Delta t}{\Delta x} \left(- \int_{x_i}^\delta s \gamma_\delta(s) ds \right) \\
&\quad - \frac{2\Delta t}{\Delta x^2} \left(\int_0^{x_i} s^2 \gamma_\delta(s) ds + x_i \int_{x_i}^\delta s \gamma_\delta(s) ds \right), \\
B_k &= \frac{\Delta t}{2\Delta x^2 (k-1)^2} \int_{(k-1)\Delta x}^{k\Delta x} s^2 \gamma_\delta(s) ds - \frac{\Delta t}{2\Delta x (k-1)} \int_{(k-1)\Delta x}^{k\Delta x} s \gamma_\delta(s) ds, \\
C_k &= \frac{\Delta t}{2\Delta x^2 (k-1)^2} \int_{(k-1)\Delta x}^{k\Delta x} s^2 \gamma_\delta(s) ds + \frac{\Delta t}{2\Delta x (k-1)} \int_{(k-1)\Delta x}^{k\Delta x} s \gamma_\delta(s) ds, \\
D &= \frac{\Delta t}{\Delta x} \int_{x_i}^\delta s \gamma_\delta(s) ds + \frac{\Delta t}{\Delta x^2} \left(\int_0^{x_i} s^2 \gamma_\delta(s) ds + x_i \int_{x_i}^\delta s \gamma_\delta(s) ds \right), \text{ and} \\
E &= \frac{\Delta t}{\Delta x^2} \left(\int_0^{x_i} s^2 \gamma_\delta(s) ds + x_i \int_{x_i}^\delta s \gamma_\delta(s) ds \right). \tag{2.46}
\end{aligned}$$

Clearly, $A + \sum_{k=\frac{x_i}{\Delta x}+1}^r (B_k + C_k) + D + E = 1$, and $B_k, C_k, D, E \geq 0$ when Δx is sufficiently small and because $-\frac{\Delta t}{2\Delta x(k-1)} \int_{(k-1)\Delta x}^{k\Delta x} s \gamma_\delta(s) ds > -\frac{\Delta t}{2(\Delta x)^2(k-1)^2} \int_{(k-1)\Delta x}^{k\Delta x} s^2 \gamma_\delta(s) ds$.

Now we want to prove that $A \geq 0$. It is equivalent to prove

$$1 - A = \frac{\Delta t}{\Delta x^2} \left[\sum_{k=\frac{x_i}{\Delta x}+1}^r \frac{1}{(k-1)^2} \int_{(k-1)\Delta x}^{k\Delta x} s^2 \gamma_\delta(s) ds + 2 \left(\int_0^{x_i} s^2 \gamma_\delta(s) ds + x_i \int_{x_i}^\delta s \gamma_\delta(s) ds \right) + \Delta x \int_{x_i}^\delta s \gamma_\delta(s) ds \right] \leq 1. \quad (2.47)$$

Notice that

$$\begin{aligned} 1 - A &= \frac{\Delta t}{\Delta x^2} \left[\sum_{k=\frac{x_i}{\Delta x}+1}^r \left(\frac{1}{(k-1)^2} \int_{(k-1)\Delta x}^{k\Delta x} s^2 \gamma_\delta(s) ds + 2x_i \int_{(k-1)\Delta x}^{k\Delta x} \left(\frac{1}{s} \right) s^2 \gamma_\delta(s) ds \right. \right. \\ &\quad \left. \left. + \Delta x \int_{(k-1)\Delta x}^{k\Delta x} \left(\frac{1}{s} \right) s^2 \gamma_\delta(s) ds \right) + 2 \int_0^{x_i} s^2 \gamma_\delta(s) ds \right] \\ &\leq \frac{\Delta t}{\Delta x^2} \left[\sum_{k=\frac{x_i}{\Delta x}+1}^r \left(\frac{1}{(k-1)^2} \int_{(k-1)\Delta x}^{k\Delta x} s^2 \gamma_\delta(s) ds + \frac{2x_i}{(k-1)\Delta x} \int_{(k-1)\Delta x}^{k\Delta x} s^2 \gamma_\delta(s) ds \right. \right. \\ &\quad \left. \left. + \frac{\Delta x}{(k-1)\Delta x} \int_{(k-1)\Delta x}^{k\Delta x} s^2 \gamma_\delta(s) ds \right) + 2 \int_0^{x_i} s^2 \gamma_\delta(s) ds \right] \\ &\leq \frac{\Delta t}{\Delta x^2} \left[\sum_{k=\frac{x_i}{\Delta x}+1}^r 4 \int_{(k-1)\Delta x}^{k\Delta x} s^2 \gamma_\delta(s) ds + 4 \int_0^{x_i} s^2 \gamma_\delta(s) ds \right] \\ &= 4 \frac{\Delta t}{\Delta x^2} \left[\sum_{k=\frac{x_i}{\Delta x}+1}^r \int_{(k-1)\Delta x}^{k\Delta x} s^2 \gamma_\delta(s) ds + \int_0^{x_i} s^2 \gamma_\delta(s) ds \right] = \frac{4\Delta t}{\Delta x^2} \int_0^\delta s^2 \gamma_\delta(s) ds \\ &= 4 \frac{\Delta t}{\Delta x^2} \leq 1. \end{aligned}$$

Since $\frac{\Delta t}{\Delta x^2} \leq \frac{1}{4}$, so $1 - A \leq 1$. Therefore,

$$A \geq 0 \text{ for } B_k \geq \frac{\Delta t}{2\Delta x^2(k-1)^2} \int_{(k-1)\Delta x}^{k\Delta x} s^2 \gamma_\delta(s) ds - \frac{\Delta t}{2\Delta x^2(k-1)^2} \int_{(k-1)\Delta x}^{k\Delta x} s^2 \gamma_\delta(s) ds = 0.$$

Summarizing the coefficients of equation (2.45) gives

- $A, B_k, C_k, D, E \geq 0$
- $A + \sum_{k=\frac{x_i}{\Delta x}+1}^r (B_k + C_k) + D + E = 1.$

Hence $u_i^{m+1} \leq \left(A + \sum_{k=\frac{x_i}{\Delta x}+1}^r (B_k + C_k) + D + E \right) M = M$.

Case III Local: Consider $i \in \{N + r + 1, \dots, 2N - 1\}$ which is the local region. Then

$$u_i^{m+1} = u_i^m + \frac{\Delta t}{\Delta x^2} \left(u_{i+1}^m - 2u_i^m + u_{i-1}^m \right) + \Delta t f_i^m \leq \left(1 - \frac{2\Delta t}{\Delta x^2} \right) u_i^m + \frac{\Delta t}{\Delta x^2} \left(u_{i+1}^m + u_{i-1}^m \right)$$

with $\frac{\Delta t}{\Delta x^2} \leq \frac{1}{4}$ which gives all positive coefficients, so $u_i^{m+1} \leq M$.

Combining case I, II, III we can conclude that given $u_i^m \leq M$ for all $i \in I_\Omega$, and $\frac{\Delta t}{\Delta x^2} \leq \frac{1}{4}$ we have $u_i^{m+1} \leq M$ for all $i \in I_\Omega$. According to induction, the theorem is proved. □

Corollary 2. Suppose for $i \in I = I_\Omega \cup I_B$, $n = 0, 1, \dots, N_T - 1$, and $T = N_T \cdot \Delta t$ that $\{u_i^n\}$ solves the following discrete QNL diffusion equation (2.40) then we have the following upper bound for u_i^n given that $\frac{\Delta t}{\Delta x^2} \leq \frac{1}{4}$,

$$u_i^n \leq T \cdot \|f\|_{\ell^\infty(I)} + \max\{\|g_i^0\|_{\ell^\infty(I)}, \|q_i^n\|_{\ell^\infty(I_B)}\}. \quad (2.48)$$

Proof. We introduce a comparison function

$$w_i^n = u_i^n + (T - n \cdot \Delta t) \|f\|_{\ell^\infty(I)} \geq u_i^n \quad (2.49)$$

for $i \in I$, and $n \geq 0$. Then we have

$$\frac{w_i^{n+1} - w_i^n}{\Delta t} = \frac{u_i^{n+1} - u_i^n}{\Delta t} - \|f\|_{\ell^\infty(I)} = \mathcal{L}_{\delta, \Delta x}^{qnl} u_i^n + \left(f_i^n - \|f\|_{\ell^\infty(I)} \right)$$

where $\left(f_i^n - \|f\|_{\ell^\infty(I)} \right) \leq 0$. Therefore by Theorem 8, w_i^n satisfies the discrete maximum principle $w_i^n \leq \max\{w_i^0 |_{i \in I}, w_i^n |_{i \in I_B}\}$ for all $i \in I_\Omega$ and $n \geq 0$, given that $\frac{\Delta t}{\Delta x^2} \leq \frac{1}{4}$.

Notice that

$$w_i^0 = u_i^0 + T \cdot \|f\|_{\ell^\infty(I)} \leq \max\{\|g_i^0\|_{\ell^\infty(I)}, \|q_i^n\|_{\ell^\infty(I_B)}\} + T \cdot \|f\|_{\ell^\infty(I)} \quad (2.50)$$

and also that

$$w_i^n|_{i \in I_B} = u_i^n|_{i \in I_B} + \left(T - n \cdot \Delta t\right) \|f\|_{\ell^\infty(I)} \leq \max\{\|g_i^0\|_{\ell^\infty(I)}, \|q_i^n\|_{\ell^\infty(I_B)}\} + T \cdot \|f\|_{\ell^\infty(I)}. \quad (2.51)$$

combined with the fact that $u_i^n|_{i \in I} \leq w_i^n|_{i \in I}$ proves the corollary. \square

Remark 3. *Although in the proof of the stability analysis, we require that $\frac{\Delta t}{\Delta x^2} \leq \frac{1}{4}$ to proceed with the analysis; meanwhile, we notice in the simulation that with $\frac{\Delta t}{\Delta x^2}$ close to $\frac{1}{2}$, we still have stable numerical results.*

2.4 Convergence of Discretized Quasi-nonlocal Operator

In this section, we prove the convergence results of the proposed FDM scheme.

Theorem 9. Global error estimate of the discrete solution *Suppose $u(x, t)$ is the strong solution to (2.4) and u_i^n is the discrete solution to the scheme (2.7) with $i \in I, n = 0, 1, \dots, N_T - 1$, and $N_T \Delta t = T$, respectively. Then we have*

$$|u(x_i, t^n) - u_i^n| \leq T \cdot C_\delta(\Delta x + \Delta t) \quad (2.52)$$

given that $\frac{\Delta t}{\Delta x^2} \leq \frac{1}{4}$.

Proof. We define $e_i^n = u(x_i, t^n) - u_i^n$, $i = 1, 2, \dots, 2N - 1$, $n = 0, 1, \dots, N_T$ to be the error between the exact and discrete solutions. Then from the consistency analysis, and since $f_i^n = f(x_i, t^n)$, we have that

$$\begin{cases} \frac{e_i^{n+1} - e_i^n}{\Delta t} - \mathcal{L}_{\delta, \Delta x}^{qnl} e_i^n = \varepsilon_{c,i}, & \text{for } i \in I_\Omega, \text{ and } n \geq 0 \\ e_i^0 = 0, i \in I & \text{(Initial Error)} \\ e_i^n = 0, i \in I_B & \text{(Boundary Error)} \end{cases} \quad (2.53)$$

where $|\varepsilon_{c,i}| < C_\delta(\Delta x + \Delta t)$ according to the consistency analysis. Hence we consider the following auxiliary function

$$w_i^n = e_i^n - (n\Delta t) \cdot C_\delta(\Delta x + \Delta t). \quad (2.54)$$

Observe that

$$\begin{aligned} & \frac{w_i^{n+1} - w_i^n}{\Delta t} - \mathcal{L}_{\delta, \Delta x}^{qnl} w_i^n \\ &= \frac{[e_i^{n+1} - C_\delta(\Delta x + \Delta t)((n+1)\Delta t)] - [e_i^n - C_\delta(\Delta x + \Delta t)(n\Delta t)]}{\Delta t} - \mathcal{L}_{\delta, \Delta x}^{qnl} e_i^n \\ &= \frac{e_i^{n+1} - e_i^n}{\Delta t} - C_\delta(\Delta x + \Delta t) - \mathcal{L}_{\delta, \Delta x}^{qnl} e_i^n \\ &= \varepsilon_{c,i} - C_\delta(\Delta x + \Delta t) \leq 0. \end{aligned} \quad (2.55)$$

Then w_i^n satisfies

$$\begin{cases} \frac{w_i^{n+1} - w_i^n}{\Delta t} - \mathcal{L}_{\delta, \Delta x}^{qnl} w_i^n \leq 0, & i \in I_\Omega, \\ w_i^0 = 0, & i \in I, \quad \text{(Initial)}, \\ w_i^n = -(n\Delta t) \cdot C_\delta(\Delta x + \Delta t), & i \in I_B \quad \text{(Boundary)}, \end{cases} \quad (2.56)$$

because of the the discrete maximum principle proved in Theorem 8, so

$$w_i^n \leq \max\{w_i^0 | i \in I, w_i^n |_{i \in I_B}\} = 0, \quad \forall i \in I_\Omega. \quad (2.57)$$

Therefore, $e_i^n \leq (n\Delta t) \cdot C_\delta(\Delta x + \Delta t)$. Similarly when $w_i^n = e_i^n + (n\Delta t) \cdot C_\delta(\Delta x + \Delta t)$

we have $e_i^n \geq -(n\Delta t) \cdot C_\delta(\Delta x + \Delta t)$. Hence, $|e_i^n| \leq (n\Delta t) \cdot C_\delta(\Delta x + \Delta t)$ which gives $|u(x_i, t^n) - u_i^n| \leq T \cdot C_\delta(\Delta x + \Delta t)$.

□

2.5 Study of the Courant-Friedricks-Lewy (CFL) Condition

In this section, we study the CFL condition of the new finite difference scheme by employing the Von Neumann stability analysis. We denote $\frac{\Delta t}{\Delta x}$ by λ_1 and $\frac{\Delta t}{(\Delta x)^2}$ by λ_2 and insert $u_i^n = (g(\theta))^n e^{\sqrt{-1}\theta x_i}$ into the scheme (2.6) where θ is a given wave number. We have the following three cases:

- **Case I Nonlocal:** for $x_i \leq 0$, the growth factor is

$$g(\theta) = 1 + \lambda_2 \sum_{j=1}^r \frac{2(\cos(\theta j \Delta x) - 1)}{j^2} \int_{(j-1)\Delta x}^{j\Delta x} s^2 \gamma_\delta(s) ds. \quad (2.58)$$

- **Case II Transitional:** for $0 < x_i \leq \delta$, the growth factor is

$$\begin{aligned} g(\theta) = & 1 + \lambda_1 \sum_{j=\frac{x_i}{\Delta x}+1}^r \frac{(\cos(\theta(j-1)\Delta x) - 1)}{(j-1)} \int_{(j-1)\Delta x}^{j\Delta x} s \gamma_\delta(s) ds \\ & - \lambda_1 \sum_{j=\frac{x_i}{\Delta x}+1}^r \frac{\sqrt{-1} \sin(\theta(j-1)\Delta x)}{(j-1)} \int_{(j-1)\Delta x}^{j\Delta x} s \gamma_\delta(s) ds \\ & + \lambda_1 \left(\int_{x_i}^{\delta} s \gamma_\delta(s) ds \right) (\cos(\theta \Delta x) + \sqrt{-1} \sin(\theta \Delta x) - 1) \\ & + \lambda_2 \left(\int_0^{x_i} s^2 \gamma_\delta(s) ds + x_i \int_{x_i}^{\delta} s \gamma_\delta(s) ds \right) (2 \cos(\theta \Delta x) - 2). \end{aligned} \quad (2.59)$$

- **Case III Local:** for $x_i > \delta$, the growth factor is

$$g(\theta) = 1 + \lambda_2 (2 \cos(\theta \Delta x) - 2). \quad (2.60)$$

Proof. Performing the Von Neumann analysis for stability we substitute $u_i^n = (g(\theta))^n e^{\sqrt{-1}\theta x_i}$

Case I:

$$\frac{u_i^{n+1} - u_i^n}{\Delta t} = \sum_{j=1}^r \frac{u_{i+j}^n - 2u_i^n + u_{i-j}^n}{(j\Delta x)^2} \int_{(j-1)\Delta x}^{j\Delta x} s^2 \gamma_\delta(s) ds \quad (2.61)$$

Substituting $u_i^n = (g(\theta))^n e^{\sqrt{-1}\theta x_i}$ gives

$$g(\theta)^n e^{\sqrt{-1}\theta x_i} (g(\theta) - 1) = \lambda_2 \sum_{j=1}^r \frac{g(\theta)^n e^{\sqrt{-1}\theta x_i} (e^{\sqrt{-1}\theta \Delta x} - 2 + e^{-\sqrt{-1}\theta \Delta x})}{j^2} \int_{(j-1)\Delta x}^{j\Delta x} s^2 \gamma_\delta(s) ds. \quad (2.62)$$

Therefore, we can conclude the growth factor for the nonlocal region is

$$g(\theta) = 1 + \lambda_2 \sum_{j=1}^r \left(\frac{2(\cos(\theta j \Delta x) - 1)}{j^2} \int_{(j-1)\Delta x}^{j\Delta x} s^2 \gamma_\delta(s) ds \right). \quad (2.63)$$

Case II:

$$\begin{aligned} \frac{u_i^{n+1} - u_i^n}{\Delta t} &= \sum_{j=\frac{x_i}{\Delta x}+1}^r \frac{u_{i+j-1}^n - 2u_i^n + u_{i-j+1}^n}{2(j-1)\Delta x} \int_{(j-1)\Delta x}^{j\Delta x} s \gamma_\delta(s) ds \\ &\quad - \sum_{j=\frac{x_i}{\Delta x}+1}^r \frac{u_{i+j-1}^n - u_{i-j+1}^n}{2(j-1)\Delta x} \int_{(j-1)\Delta x}^{j\Delta x} s \gamma_\delta(s) ds \\ &\quad + \left(\int_{x_i}^{\delta} s \gamma_\delta(s) ds \right) \frac{u_{i+1}^n - u_i^n}{\Delta x} \\ &\quad + \left(\int_0^{x_i} s^2 \gamma_\delta(s) ds + x_i \int_{x_i}^{\delta} s \gamma_\delta(s) ds \right) \frac{u_{i+1}^n - 2u_i^n + u_{i-1}^n}{(\Delta x)^2}. \end{aligned} \quad (2.64)$$

Similarly to the nonlocal region substituting $u_i^n = (g(\theta))^n e^{\sqrt{-1}\theta x_i}$ gives

$$\begin{aligned}
& g(\theta)^n e^{\sqrt{-1}\theta x_i} (g(\theta) - 1) = \\
& \lambda_1 \sum_{j=\frac{x_i}{\Delta x}+1}^r \frac{1}{2(j-1)} \left(g(\theta)^n e^{\sqrt{-1}\theta x_i} (e^{\sqrt{-1}\theta(j-1)\Delta x} - 2 + e^{-\sqrt{-1}\theta(j-1)\Delta x}) \right) \int_{(j-1)\Delta x}^{j\Delta x} s\gamma_\delta(s) ds \\
& - \lambda_1 \sum_{j=\frac{x_i}{\Delta x}+1}^r \frac{1}{2(j-1)} \left(g(\theta)^n e^{\sqrt{-1}\theta x_i} (e^{\sqrt{-1}\theta(j-1)\Delta x} - e^{-\sqrt{-1}\theta(j-1)\Delta x}) \right) \int_{(j-1)\Delta x}^{j\Delta x} s\gamma_\delta(s) ds \\
& + \lambda_1 \left(\int_{x_i}^{\delta} s\gamma_\delta(s) ds \right) \left(g(\theta)^n e^{\sqrt{-1}\theta x_i} (e^{\sqrt{-1}k\Delta x} - 1) \right) \\
& + \lambda_2 \left(\int_0^{x_i} s^2\gamma_\delta(s) ds + x_i \int_{x_i}^{\delta} s\gamma_\delta(s) ds \right) \left(g(\theta)^n e^{\sqrt{-1}\theta x_i} (e^{\sqrt{-1}\theta\Delta x} - 2 + e^{-\sqrt{-1}\theta\Delta x}) \right).
\end{aligned} \tag{2.65}$$

Therefore, we can conclude the growth factor for the transitional region is

$$\begin{aligned}
g(\theta) &= 1 + \lambda_1 \sum_{j=\frac{x_i}{\Delta x}+1}^r \frac{(\cos(\theta(j-1)\Delta x) - 1)}{(j-1)} \int_{(j-1)\Delta x}^{j\Delta x} s\gamma_\delta(s) ds \\
& - \lambda_1 \sum_{j=\frac{x_i}{\Delta x}+1}^r \frac{\sqrt{-1}\sin(\theta(j-1)\Delta x)}{(j-1)} \int_{(j-1)\Delta x}^{j\Delta x} s\gamma_\delta(s) ds \\
& + \lambda_1 \left(\int_{x_i}^{\delta} s\gamma_\delta(s) ds \right) (\cos(\theta\Delta x) + \sqrt{-1}\sin(k\Delta x) - 1) \\
& + \lambda_2 \left(\int_0^{x_i} s^2\gamma_\delta(s) ds + x_i \int_{x_i}^{\delta} s\gamma_\delta(s) ds \right) (2\cos(\theta\Delta x) - 2).
\end{aligned} \tag{2.66}$$

Case III:

$$\frac{u_i^{n+1} - u_i^n}{\Delta t} = \frac{u_{i+1}^n - 2u_i^n + u_{i-1}^n}{(\Delta x)^2} \tag{2.67}$$

Finally, substituting $u_i^n = (g(\theta))^n e^{\sqrt{-1}\theta x_i}$ gives

$$g(\theta)^n e^{\sqrt{-1}\theta x_i} (g(\theta) - 1) = \lambda_2 \left(g(\theta)^n e^{\sqrt{-1}\theta x_i} (e^{\sqrt{-1}\theta\Delta x} - 2 + e^{-\sqrt{-1}k\Delta x}) \right). \tag{2.68}$$

Therefore, we can conclude the growth factor for the local region is

$$g(\theta) = 1 + \lambda_2(2 \cos(\theta\Delta x) - 2). \quad (2.69)$$

Clearly, we have $\lambda_2 = \Delta x\lambda_1$, so once we get the CFL constraint on λ_1 , the CFL condition for λ_2 will be satisfied when Δx is sufficiently small. Because it is very difficult to analytically find this upper bound we implement the growth factor $g(\theta)$ numerically to identify restrictions on λ_1 and λ_2 to ensure $|g(\theta)| \leq 1$. \square

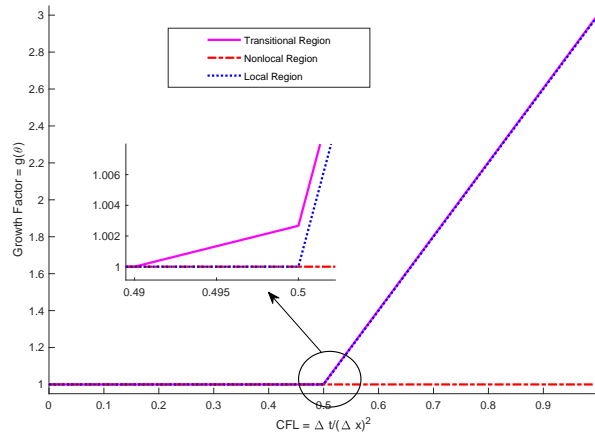


Figure 2.3: Maximum Growth Rate of (2.58), (2.59), (2.60) for the new finite difference method versus that of (2.8) for the original finite difference method.

For linear local diffusion models with explicit Euler integration and the middle-point finite-difference discretization, the CFL is restricted by $\text{CFL} = \frac{\Delta t}{\Delta x^2} \leq 0.5$. This provides the largest step size in time to reduce computational cost while preserves stability. By numerically analyzing the growth factor in Figure 2.3, we found that the nonlocal and local regions match the typical restrictions for stability, but the transitional region is slightly less than 0.5. This factor needs to be considered for stability restrictions to the CFL on the whole coupling system. On the other hand, compared with the original FDM scheme proposed in [15], the new FDM discretization can afford a larger CFL condition, which suggests that the new scheme is more stable.

2.6 Numerical Examples

In this section, we test several numerical examples to confirm the stability and convergence results. We fix the nonlocal diffusion kernel to be a constant kernel

$$\gamma_\delta(s) = \frac{3}{\delta^3} \chi_{[-\delta, \delta]}(s).$$

1. For the first example, we consider the asymptotic compatibility (AC) of the discretized operator $\mathcal{L}_{\delta, \Delta x}^{qnl}$ to the local diffusion problem as the horizon δ and spatial discretization Δx go to zero at the same time.

We consider the external force f as

$$f(x, t) = 30x^4 e^{-t} + e^{-t}(x^6 - 1) + 2. \quad (2.70)$$

Then, the exact solution to the local diffusion $u_t^\ell = u_{xx}^\ell + f$ with $u^\ell(-1, t) = u^\ell(1, t) = 0$ and $u^\ell(x, 0) = (1 - x^2) - (x^6 - 1)$ is

$$u^\ell(x, t) = (1 - x^2) - e^{-t}(x^6 - 1). \quad (2.71)$$

To test the AC convergence, we fix $\delta = r\Delta x$ with $r = 3$ and set the CFL to be $CFL = 0.45$, that is $\Delta t = 0.2\Delta x^2$, and the termination time is chosen to be $T = 1$.

First order convergence with respect to Δx is observed. The convergence order and $L_{\Omega \times [0, T]}^\infty$ differences between $u^\ell(x, t)$ and discrete solution of $u_{\delta, \Delta x}^{qnl}$ are listed in Table 2.1. Also the visual comparison of the two solutions at $t = 0$ and $t = T$ are displayed in Figure 2.4 with good agreement.

Table 2.1: $L_{\Omega \times [0, T]}^\infty$ differences between the local continuous solution u^ℓ and discrete solution $u_{\delta, \Delta x}^{qnl}$. We fix $\delta = 3\Delta x$, and the kernel is $\gamma_\delta(s) = \frac{3}{\delta^3} \chi_{[-\delta, \delta]}(s)$. The termination time $T = 1$ and $\Delta t = 0.2\Delta x^2$.

Δx	$\ u^\ell(x_i, t^n) - u_{\delta, \Delta x}^{qnl}(x_i, t^n)\ _{L_{\Omega \times [0, T]}^\infty}$	Order
$\frac{1}{50}$	0.1422	—
$\frac{1}{100}$	7.168e-2	0.988
$\frac{1}{200}$	3.614e-2	0.988
$\frac{1}{400}$	1.820e-2	0.990
$\frac{1}{800}$	9.151e-3	0.992
$\frac{1}{1600}$	4.594e-3	0.994

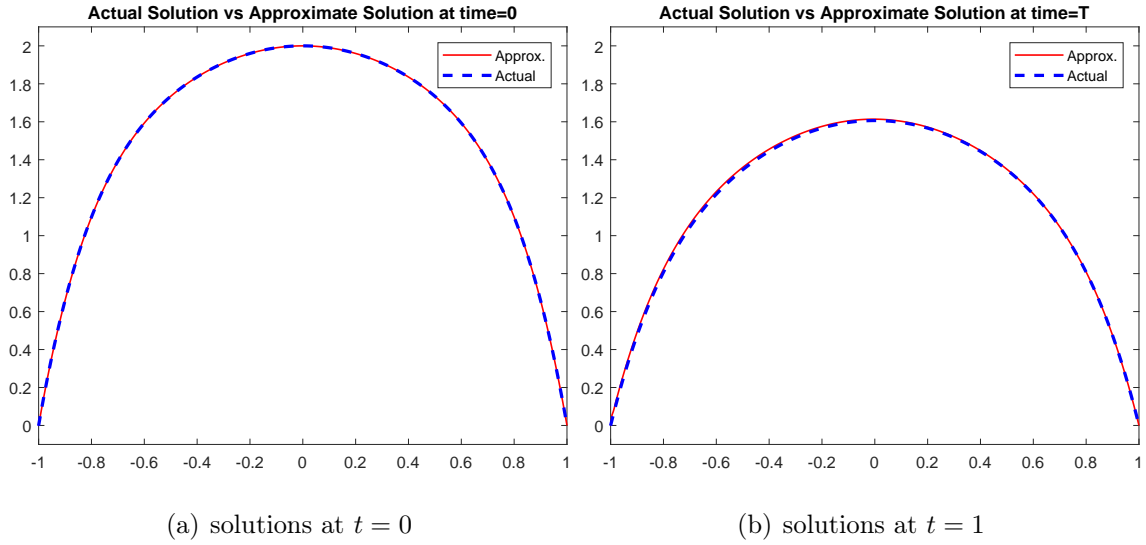


Figure 2.4: Plots of solutions to the approximate and actual solutions. The kernel function was chosen as $\gamma_\delta(s) = \frac{3}{\delta^3} \chi_{[-\delta, \delta]}(s)$. The coupling inference is at $x^* = 0$, and the mesh size is $\Delta x = \frac{1}{400}$ with a horizon as $\delta = \frac{3}{400}$, the temporal step size is $\Delta t = 0.45\Delta x^2$.

- In the following example, we compare the original scheme $\tilde{\mathcal{L}}_\delta^{qnl}$ (2.8) proposed in [15] with the new proposed scheme $\mathcal{L}_{\delta, \Delta x}^{qnl}$ in (2.6).

We are going to compare the AC convergence between (2.6) and (2.8). The exact local

continuous solution is chosen to be

$$u^\ell(x, t) = e^{-t}(1-x)^2(1+x)^2x^2 \quad (2.72)$$

and the corresponding external force is

$$\begin{aligned} f(x, t) &= u_t^\ell - u_{xx}^\ell \\ &= -e^{-t}((x-x^3)^2 + (2-24x^2+30x^4)). \end{aligned} \quad (2.73)$$

Again the kernel used is $\gamma_\delta(s) = \frac{3}{\delta^3}$ with $\delta = 3\Delta x$. We denote the solution obtained by $\mathcal{L}_{\delta, \Delta x}^{qnl}$ by $u_{\delta, \Delta x}^{qnl}$ and the solution obtained by $\tilde{\mathcal{L}}_{\delta, \Delta x}^{qnl}$ by $\tilde{u}_{\delta, \Delta x}^{qnl}$.

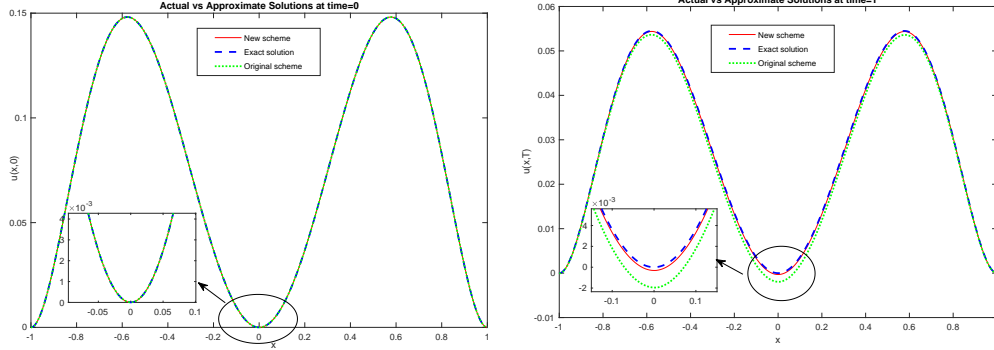
First order AC convergence with respect to Δx are observed in Table 2.2 for both schemes (2.6) and (2.8), respectively. The approximation using scheme (2.6) at larger step size has a second order convergence rate, and at smaller step size tends to be of first order.

Table 2.2: $L^\infty_{\Omega \times [0, T]}$ differences between the local continuous solution u^ℓ and two discrete solutions $u_{\delta, \Delta x}^{qnl}$, $\tilde{u}_{\delta, \Delta x}^{qnl}$ using the FDM schemes (2.6) and (2.8), respectively. We fix $\delta = 3\Delta x$, and the kernel is $\gamma_\delta(s) = \frac{3}{\delta^3}$. The termination time is $T = 1$ and $\Delta t = 0.2\Delta x^2$.

Δx	$\ u^\ell(x_i, t^n) - \tilde{u}_{\delta, \Delta x}^{qnl}(x_i, t^n)\ _{L^\infty}$	Order	$\ u^\ell(x_i, t^n) - u_{\delta, \Delta x}^{qnl}(x_i, t^n)\ _{L^\infty}$	Order
$\frac{1}{50}$	9.255e-3	—	7.200e-3	—
$\frac{1}{100}$	4.692e-3	0.980	1.698e-3	2.08
$\frac{1}{200}$	2.356e-3	0.994	4.121e-4	1.09
$\frac{1}{400}$	1.179e-3	0.998	1.931e-4	1.09
$\frac{1}{800}$	5.900e-4	0.999	9.628e-5	1.00
$\frac{1}{1600}$	2.951e-4	1.00	4.806e-5	1.00

Next, we compare the three solutions obtained from the new scheme (1), the exact local continuous solution (2), and the original scheme (3) in Figure 2.5. Notice that the exact local continuous solution $u^\ell(x, t)$ should remain non negative throughout the entire computational domain $\Omega \times [0, T]$, however, both $u_{\delta, \Delta x}^{qnl}$ and $\tilde{u}_{\delta, \Delta x}^{qnl}$ become slightly negative around the interface

$x^* = 0$. This does not contradict the discrete maximum principle of $\mathcal{L}_{\delta, \Delta x}^{qnl}$ as the external force $f(x, t)$ defined in (2.73) does not retain negativity on $[-1, 1]$ as required in the assumption of Theorem 8.



(a) solutions at $t = 0$

(b) solutions at $t = 1$

Figure 2.5: Numerical comparison between the new scheme (2.6) and original scheme (2.8) used to approximate (2.72) with external force given by (2.73). The spatial step size is $\Delta x = \frac{1}{200}$ and $\Delta t = 0.25\Delta x^2$.

2.7 New Finite Difference Scheme Conclusion

We propose a new scheme to discretize the quasi-nonlocal (QNL) coupling operator introduced in [15] for the nonlocal-to-local diffusion problem. This new finite difference approximation preserves the properties of continuous equation on a discrete level. Consistency, stability, the maximum principle and the global convergence analysis of the scheme are proved rigorously. We analytically find the CFL conditions through the Von Neumann stability analysis and numerically calculate the CFL values for a given spatial discretization. The numerical calculations of the CFL provide an additional alert around the interface when considering the temporal step size for an explicit time integrator. The CFL restrictions on the transitional region were discovered to be slightly less than $\frac{1}{2}$ with the explicit Euler method employed in a diffusion problem. Multiple numerical examples are then provided and summarized to verify the theoretical findings. A comparison with the original scheme used in [15] is also provided which confirmed the improvements of the new scheme. See this chapter in [23].

CHAPTER 3: DEVELOPMENT OF THE COEFFICIENT MATRIX, AND MORE
NUMERICAL EXAMPLES

In this chapter, we develop the coefficient matrices necessary for the finite difference scheme that couples nonlocal and local diffusion. Additionally, we investigate the effects of applying different boundary conditions, specifically Neumann and Robin boundary conditions, on the approximate solutions produced by the nonlocal to local finite difference scheme outlined in this dissertation. These boundary conditions play a crucial role in shaping the behavior of the solution near the boundaries of the domain, and their impact on the accuracy and stability of the numerical results will be explored.

To provide context, refer the diffusion equation, which serves as the foundational model for this investigation:

$$u_t(x, t) = u_{xx}(x, t) + f(x, t) \tag{3.1}$$

where, $u(x, t)$ represents the temperature distribution over time and space. In addition, recall the diffusion equation with nonlocal to local coupling operator and Dirichlet boundary conditions

$$\begin{cases} u_t(x, t) = \mathcal{L}^{nl}u(x, t) + f(x, t) & x \in [-1, 1] \\ u(x, 0) = u_0(x) & x \in (-1, 1) \\ u(x, t) = 0 & x \in \{-1\} \cup \{1\} \end{cases} \tag{3.2}$$

In the development of the coefficient matrix for the quasi-nonlocal coupling scheme, it is also useful to revisit the formulation of the 1-dimensional quasi-nonlocal energy. The quasi-nonlocal energy plays a key role in governing the behavior of the system and is integral to

constructing the finite difference scheme, as it provides a foundation for deriving the operator and ensuring consistency in the coupling between the local and nonlocal regions.

$$E^{QNL}(u) = \frac{1}{2} \iint_{x \leq \cup y \leq 0} \gamma_\delta(|y-x|)(u(y,t) - u(x,t))^2 dy dx + \frac{1}{2} \int_{x < 0} |u'(x,t)|^2 \omega_\delta(x,t) dx \quad (3.3)$$

with the weight function definition and characteristics

$$\omega_\delta(x,t) = \int_0^1 dt \int_{|s| < \frac{x}{t}} |s|^2 \gamma(|s|) ds \quad (3.4)$$

$$\omega_\delta(x,t) = 2 \int_0^x s^2 \gamma_\delta(|s|) ds + 2x \int_x^\infty s \gamma_\delta(|s|) ds \quad (3.5)$$

$$\omega'_\delta(x,t) = 2 \int_x^\infty s \gamma_\delta(s) ds, \quad (3.6)$$

and the kernel is defined as

$$\begin{cases} \gamma_\delta(|s|) = \frac{1}{\delta^3} \gamma\left(\frac{|s|}{\delta}\right), & \gamma \text{ is nonnegative and nonincreasing on } (0,1), \\ \text{with } \text{supp}(\gamma) \subset [0,1] \text{ and } \int_{-\delta}^\delta |s|^2 \gamma(|s|) ds = 2. \end{cases} \quad (3.7)$$

Finally, refer to the continuous nonlocal to local operator, which plays a fundamental role

in the coupling of local and nonlocal diffusion models.

$$\mathcal{L}^{qnl}u(x, t) = \begin{cases} 2 \int_{y \in R} \gamma_\delta(|y - x|)(u(y, t) - u(x, t))dy, & \text{if } x < 0 \\ 2 \int_{y < 0} \gamma_\delta(|y - x|) \left(u(y, t) - u(x, t) \right) dy + (\omega_\delta(x, t)u'(x, t))', & \text{if } x \in [0, \delta) \\ u''(x, t), & \text{if } x \geq \delta. \end{cases}$$

In the next section, we will derive the numerical operator from the continuous nonlocal to local operator, and subsequently develop the corresponding coefficient matrix for Dirichlet boundary conditions. This process will enable us to discretize the problem effectively, ensuring that the finite difference scheme accurately captures the behavior of the system under the specified boundary conditions.

3.1 Numerical Constants

In this section, we focus on the derivation of the numerical operator from the continuous operator and the subsequent development of the coefficient matrix for Dirichlet boundary conditions. This process begins by discretizing the continuous local-to-nonlocal operator using an appropriate finite difference scheme, transforming the continuous differential operator into its numerical counterpart. The next step involves constructing the coefficient matrix that corresponds to the discretized system under Dirichlet boundary conditions, ensuring that the boundary values are properly incorporated into the scheme. This matrix formulation is crucial for solving the system efficiently while maintaining accuracy and stability in the transition between local and nonlocal diffusion.

Theorem 10. *The following continuous operators $\mathcal{L}_\delta^{qnl}u(x, t)$ can be approximated by numerical operators $\mathcal{L}_{\delta, \Delta x}^{qnl}u_i^n$*

Nonlocal Domain

$$\begin{aligned}\mathcal{L}_\delta^{qnl}u(x, t) &= \int_{-\delta}^{\delta} \left(u(x + s, t) - u(x, t) \right) \gamma_\delta(s) ds \approx \\ \mathcal{L}_{\delta, \Delta x}^{qnl}u_i^n &= \sum_{j=1}^r \frac{\gamma \Delta x (j^3 - (j-1)^3)}{3j^2} u_{i+j}^n - \frac{2\gamma \Delta x (j^3 - (j-1)^3)}{3j^2} u_i^n + \frac{\gamma \Delta x (j^3 - (j-1)^3)}{3j^2} u_{i-j}^n\end{aligned}\tag{3.8}$$

Transitional Domain

$$\begin{aligned}
\mathcal{L}_\delta^{qnl} u(x, t) &= \int_x^\delta \gamma_\delta(s) \left(u(x-s, t) - u(x, t) \right) ds + \left(\int_x^\delta s \gamma_\delta(s) ds \right) u_x(x, t) \\
&\quad + \left(\int_0^x s^2 \gamma_\delta(s) + x \int_x^\delta s \gamma_\delta(s) ds \right) u_{xx}(x) \approx \\
\mathcal{L}_{\delta, \Delta x}^{qnl} u_i^n &= \sum_{j=\frac{x_i}{\Delta x}+1}^r (u_{i+j-1}^n - 2u_i^n + u_{i-j+1}^n) \left(\frac{\gamma \Delta x (j^2 - (j-1)^2)}{4(j-1)} \right) \\
&\quad - \sum_{j=\frac{x_i}{\Delta x}+1}^r (u_{i+j-1}^n - u_{i-j+1}^n) \left(\frac{\gamma \Delta x (j^2 - (j-1)^2)}{4(j-1)} \right) \\
&\quad + \left(\frac{\gamma(\delta^2 - x_i^2)}{2\Delta x} \right) (u_{i+1}^n - u_i^n) \\
&\quad + \left(\left(\frac{\gamma x_i^3}{3\Delta x^2} \right) + x_i \left(\frac{\gamma(\delta^2 - x_i^2)}{2\Delta x^2} \right) \right) (u_{i+1}^n - 2u_i^n + u_{i-1}^n) \tag{3.9}
\end{aligned}$$

Local Domain (Second order central difference)

$$\begin{aligned}
\mathcal{L}_\delta^{qnl} u(x, t) &= u_{xx}(x, t) = \frac{u(x_{i+1}, t^n) - 2u(x_i, t^n) + u(x_{i-1}, t^n)}{\Delta x^2} \approx \\
\mathcal{L}_{\delta, \Delta x}^{qnl} u_i^n &= \frac{1}{\Delta x^2} u_{i-1}^n - \frac{2}{\Delta x^2} u_i^n + \frac{1}{\Delta x^2} u_{i+1}^n \tag{3.10}
\end{aligned}$$

Proof. Nonlocal Domain: Symmetry of $u(x, t)$ gives the following rearrangement of the continuous operator

$$\begin{aligned}
\mathcal{L}_\delta^{qnl} u(x, t) &= \int_{-\delta}^\delta \left(u(x+s, t) - u(x, t) \right) \gamma_\delta(s) ds \\
&= 2 \int_0^\delta \gamma_\delta(s) \left(u(x+s, t) - u(x, t) \right) ds \\
&= \int_0^\delta \gamma_\delta(s) \left(2u(x+s, t) - 2u(x, t) \right) ds \\
&= \int_0^\delta \gamma_\delta(s) \left(u(x+s, t) - 2u(x, t) + u(x-s, t) \right) ds \tag{3.11}
\end{aligned}$$

Next we discretize the continuous model such that

$$\begin{aligned}
\mathcal{L}_\delta^{qnl} u(x, t) &\approx \sum_{j=1}^r \int_{(j-1)\Delta x}^{j\Delta x} s^2 \gamma_\delta(s) \left(\frac{u(x+s, t) - 2u(x, t) + u(x-s, t)}{s^2} \right) ds \\
&= \sum_{j=1}^r \frac{u(x_{i+j}, t^n) - 2u(x_i, t^n) + u(x_{i-j}, t^n)}{(j\Delta x)^2} \int_{(j-1)\Delta x}^{j\Delta x} s^2 \gamma_\delta(s) ds \\
&= \sum_{j=1}^r \frac{u_{i+j}^n - 2u_i^n + u_{i-j}^n}{(j\Delta x)^2} \left(\frac{1}{3} s^3 \gamma|_{(j-1)\Delta x}^{j\Delta x} \right) \\
&= \sum_{j=1}^r \frac{u_{i+j}^n - 2u_i^n + u_{i-j}^n}{(j\Delta x)^2} \left(\frac{1}{3} \Delta x^3 \gamma \left(j^3 - (j-1)^3 \right) \right) \\
&= \sum_{j=1}^r \frac{\gamma \Delta x (j^3 - (j-1)^3)}{3j^2} u_{i+j}^n - \frac{2\gamma \Delta x (j^3 - (j-1)^3)}{3j^2} u_i^n + \frac{\gamma \Delta x (j^3 - (j-1)^3)}{3j^2} u_{i-j}^n \\
&= \mathcal{L}_{\delta, \Delta x}^{qnl} u_i^n
\end{aligned} \tag{3.12}$$

Transitional Domain:

$$\begin{aligned}
\mathcal{L}_\delta^{qnl} u(x, t) &= \int_x^\delta \gamma_\delta(s) \left(u(x-s, t) - u(x, t) \right) ds + \left(\int_x^\delta s \gamma_\delta(s) ds \right) u_x(x, t) \\
&+ \left(\int_0^x s^2 \gamma_\delta(s) ds + x \int_x^\delta s \gamma_\delta(s) ds \right) u_{xx}(x) \\
&= \sum_{j=\frac{x_i}{\Delta x}+1}^r \frac{u_{i+j-1}^n - 2u_i^n + u_{i-j+1}^n}{2(j-1)\Delta x} \int_{(j-1)\Delta x}^{j\Delta x} s \gamma_\delta(s) ds \\
&- \sum_{j=\frac{x_i}{\Delta x}+1}^r \frac{u_{i+j-1}^n - u_{i-j+1}^n}{2(j-1)\Delta x} \int_{(j-1)\Delta x}^{jh} s \gamma_\delta(s) ds \\
&+ \left(\int_{x_i}^\delta s \gamma_\delta(s) ds \right) \frac{u_{i+1}^n - u_i^n}{\Delta x} \\
&+ \left(\int_0^{x_i} s^2 \gamma_\delta(s) ds + x_i \int_{x_i}^\delta s \gamma_\delta(s) ds \right) \frac{u_{i+1}^n - 2u_i^n + u_{i-1}^n}{(\Delta x)^2}.
\end{aligned} \tag{3.13}$$

Then the discretized continuous operator can be written as

$$\begin{aligned}
\mathcal{L}_\delta^{qnl} u(x, t) &\approx \sum_{j=\frac{x_i}{\Delta x}+1}^r \frac{u_{i+j-1}^n - 2u_i^n + u_{i-j+1}^n}{2(j-1)\Delta x} \left(\frac{s^2\gamma}{2} \Big|_{(j-1)\Delta x}^{j\Delta x} \right) \\
&- \sum_{j=\frac{x_i}{\Delta x}+1}^r \frac{u_{i+j-1}^n - u_{i-j+1}^n}{2(j-1)\Delta x} \left(\frac{s^2\gamma}{2} \Big|_{(j-1)\Delta x}^{j\Delta x} \right) \\
&+ \left(\frac{s^2\gamma}{2} \Big|_{x_i}^\delta \right) \frac{u_{i+1}^n - u_i^n}{\Delta x} \\
&+ \left(\left(\frac{s^3\gamma}{3} \Big|_0^{x_i} \right) + x_i \left(\frac{s^2\gamma}{2} \Big|_{x_i}^\delta \right) \right) \frac{u_{i+1}^n - 2u_i^n + u_{i-1}^n}{(\Delta x)^2} \\
&= \sum_{j=\frac{x_i}{\Delta x}+1}^r (u_{i+j-1}^n - 2u_i^n + u_{i-j+1}^n) \left(\frac{\gamma\Delta x(j^2 - (j-1)^2)}{4(j-1)} \right) \\
&- \sum_{j=\frac{x_i}{\Delta x}+1}^r (u_{i+j-1}^n - u_{i-j+1}^n) \left(\frac{\gamma\Delta x(j^2 - (j-1)^2)}{4(j-1)} \right) \\
&+ \left(\frac{\gamma(\delta^2 - x_i^2)}{2\Delta x} \right) (u_{i+1}^n - u_i^n) \\
&+ \left(\left(\frac{\gamma x_i^3}{3\Delta x^2} \right) + x_i \left(\frac{\gamma(\delta^2 - x_i^2)}{2\Delta x^2} \right) \right) (u_{i+1}^n - 2u_i^n + u_{i-1}^n) \\
&= \mathcal{L}_{\delta, \Delta x}^{qnl} u_i^n \tag{3.14}
\end{aligned}$$

Note: In all analyses, the radius $r = 3$ is used consistently. As a result, there are always exactly three nodes within the transition region, regardless of the size of the domain or the step size used in the finite difference scheme. This fixed radius ensures a uniform treatment of the transition region between the local and nonlocal models, simplifying the analysis while maintaining consistency across different configurations.

Local Domain: By second order central finite difference

$$\begin{aligned}
\mathcal{L}_\delta^{qnl} u(x, t) &= u_{xx}(x, t) = \frac{u(x_{i+1}, t^n) - 2u(x_i, t^n) + u(x_{i-1}, t^n)}{\Delta x^2} \approx \\
&= \frac{1}{\Delta x^2} u_{i-1}^n - \frac{2}{\Delta x^2} u_i^n + \frac{1}{\Delta x^2} u_{i+1}^n \\
&= \mathcal{L}_{\delta, \Delta x}^{qnl} u_i^n
\end{aligned} \tag{3.15}$$

□

We establish that $r = 3$, which defines the number of nodes in the transition region. From this, we derive that $\delta = r\Delta x = 3\Delta x$, where Δx is the spatial step size. The parameter γ , which is related to the interaction strength in the nonlocal model, is given by:

$$\gamma = \frac{3}{\delta^3} = \frac{3}{r^3 \Delta x^3}.$$

Next, we define the **nonlocal region constant** by

$$\begin{aligned}
\mathcal{L}^{\text{NL}} u(x, t) &= \sum_{j=1}^r \frac{\gamma \Delta x (j^3 - (j-1)^3)}{3j^2} u_{i+j}^n - \frac{2\gamma \Delta x (j^3 - (j-1)^3)}{3j^2} u_i^n + \frac{\gamma \Delta x (j^3 - (j-1)^3)}{3j^2} u_{i-j}^n \\
&= \sum_{j=1}^r \left(\frac{3j^2 + 3j + 1}{r^3 \Delta x^2 j^2} \right) u_{i+j}^n + \left(\frac{-2(3j^2 + 3j + 1)}{r^3 \Delta x^2 j^2} \right) u_i^n + \left(\frac{3j^2 + 3j + 1}{r^3 \Delta x^2 j^2} \right) u_{i-j}^n.
\end{aligned} \tag{3.16}$$

Then we define the **transitional region constants** by

$$\begin{aligned}
\mathcal{L}^{\mathbf{T}}u(x, t) &= \sum_{j=\frac{x_i}{\Delta x}+1}^r (u_{i+j-1}^n - 2u_i^n + u_{i-j+1}^n) \left(\frac{\gamma \Delta x (j^2 - (j-1)^2)}{4(j-1)} \right) \\
&\quad - \sum_{j=\frac{x_i}{\Delta x}+1}^r (u_{i+j-1}^n - u_{i-j+1}^n) \left(\frac{\gamma \Delta x (j^2 - (j-1)^2)}{4(j-1)} \right) \\
&\quad + \left(\frac{\gamma(\delta^2 - x_i^2)}{2\Delta x} \right) (u_{i+1}^n - u_i^n) \\
&\quad + \left(\left(\frac{\gamma x_i^3}{3\Delta x^2} \right) + x_i \left(\frac{\gamma(\delta^2 - x_i^2)}{2\Delta x^2} \right) \right) (u_{i+1}^n - 2u_i^n + u_{i-1}^n) \\
&= \sum_{j=\frac{x_i}{\Delta x}+1}^r (u_{i+j-1}^n - 2u_i^n + u_{i-j+1}^n) \left(\frac{3(2j-1)}{4r^3 \Delta x^2 (j-1)} \right) \text{ Nonlocal Gradient Constant} \\
&\quad - \sum_{j=\frac{x_i}{\Delta x}+1}^r (u_{i+j-1}^n - u_{i-j+1}^n) \left(\frac{3(2j-1)}{4r^3 \Delta x^2 (j-1)} \right) \text{ Nonlocal Gradient Constant} \\
&\quad + \left(\frac{3}{2\delta \Delta x} \left(1 - \left(\frac{x_i}{\delta} \right)^2 \right) \right) (u_{i+1}^n - u_i^n) \text{ Local Gradient Constant} \\
&\quad + \left(-\frac{1}{2} \left(\frac{x_i}{\delta} \right)^3 + \frac{3}{2} \left(\frac{x_i}{\delta} \right) \right) (u_{i+1}^n - 2u_i^n + u_{i-1}^n) \text{ Local Diffusion Constant.} \quad (3.17)
\end{aligned}$$

Finally, we define the **local region constant** by

$$\mathcal{L}^{\mathbf{L}} = \frac{1}{\Delta x^2} u_{i-1}^n - \frac{2}{\Delta x^2} u_i^n + \frac{1}{\Delta x^2} u_{i+1}^n. \quad (3.18)$$

The spatial index N determines the step size, with $\Delta x = \frac{1}{N}$. This step size governs the discretization of the domain, which consists of a total of $2N + r$ nodes, distributed across the different sections of the domain.

Thus, for a domain $(-1 - \delta, 1]$, or any domain using this partitioning scheme, the node distribution ensures proper handling of both local and nonlocal regions, with the transition region providing a smooth connection between them. The total number of nodes reflects the combination of these sections, providing a structured framework for the finite difference scheme used in the analysis.

This represents the general structure of the coefficient matrix for the previous numerical examples under Dirichlet boundary conditions. The matrix incorporates the nonlocal, transitional, and local diffusion constants while accounting for the boundary conditions, where $u(x, t) = 0$ on the boundary. As a result, the boundary nodes are either adjusted, leading to a reduced matrix that governs the internal nodes within the domain.

In previous works such as [35] and [49], studies examined non-Dirichlet boundary conditions. To gain a broader understanding of how the non local to local finite difference scheme applies to diffusion problems, we extended our analysis to include non-Dirichlet boundary conditions as well. The next two sections address the development of the coefficient matrix for the local to nonlocal diffusion finite difference scheme under Neumann and Robin boundary conditions.

Referring back to Theorem 5, the continuous local to nonlocal operator was derived using energy variation. This continuous operator was then transformed into the numerical operator used throughout this study. When Neumann or Robin boundary conditions are applied instead of Dirichlet conditions, we find that Neumann and Robin boundary conditions alter the operator. These modifications will be explored further, detailing their impact on the construction of the coefficient matrix and the behavior of the numerical solution.

3.2 Neumann Boundary Conditions Numerical Example

In this section, we will examine the Neumann boundary condition problem for the nonlocal to local coupling model. This analysis will focus on how the Neumann boundary conditions impact the transition between local and nonlocal diffusion within the finite difference scheme, and the structure of the coefficient matrix.

Using the same definitions and conditions described in the previous section, we proceed with

the Neumann boundary condition problem

$$\begin{cases} u_t(x, t) = \mathcal{L}^{qnl}u(x, t) + f(x, t) & x \in [-1, 1] \\ u(x, 0) = u_0(x) & x \in (-1, 1) \\ u_x(x, t) = 0 & x \in \{-1\} \cup \{1\}. \end{cases}$$

The Neumann boundary conditions and definition of $u_x(x, t)$ give

$$u_x(-1 - 3\Delta x, t) = u_x(-1 - 2\Delta x, t) = u_x(-1 - \Delta x, t) = u_x(-1, t) = u_x(1, t) = 0 \quad (3.19)$$

which have nodal placement at

$$u_x(x_1, t) = u_x(x_2, t) = u_x(x_3, t) = u_x(x_4, t) = u_x(x_{2N+r+1}, t) = 0, \quad (3.20)$$

and

$$u_x(x, t) = \frac{u(x + \Delta x, t) - u(x, t)}{\Delta x}. \quad (3.21)$$

Then

$$u_x(x_1, t) = \frac{u(x_2, t) - u(x_1, t)}{\Delta x} = 0 \quad (3.22)$$

which gives

$$-u_1 + u_2 = 0. \quad (3.23)$$

Similarly,

$$\begin{aligned} -u_2 + u_3 &= 0 \\ -u_3 + u_4 &= 0 \\ -u_4 + u_5 &= 0 \\ -u_{2N+r} + u_{2N+r-1} &= 0. \end{aligned} \quad (3.24)$$

Neumann Boundary Condition Problem Numerical Example:

Let $N = 800$.

Exact Solution: $u(x, t) = (1 - x^2)^2 e^{-t}$

Force Function: $u_t = u_{xx} + f$, so $f(x, t) = -(1 - x^2)^2 e^{-t} - 4e^{-t}(3x^2 - 1)$

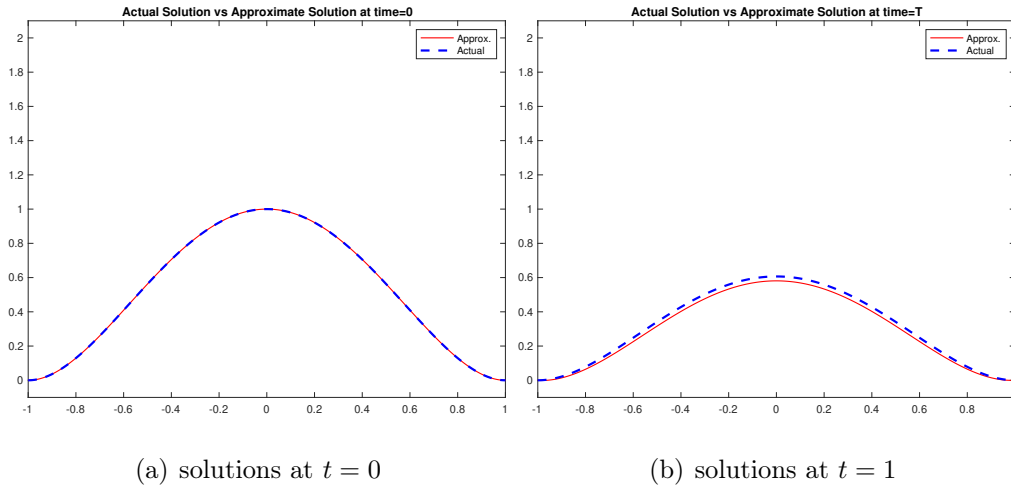


Figure 3.1: Numerical comparison between approximate and actual solution with Neumann Boundary Conditions

Convergence with respect to Δx is not observed. The convergence order and $L^\infty_{\Omega \times [0, T]}$ differences between $u^\ell(x, t)$ and discrete solution of $u_{\delta, \Delta x}^{qnl}$ are listed in Table 3.1. Also the visual comparison of the two solutions at $t = 0$ and $t = T$ are displayed in Figure 3.1 with good agreement.

Table 3.1: $L_{\Omega \times [0, T]}^\infty$ differences between the local continuous solution u^ℓ and discrete solution $u_{\delta, \Delta x}^{qnl}$. We fix $\delta = 3\Delta x$, and the kernel is $\gamma_\delta(s) = \frac{3}{\delta^3} \chi_{[-\delta, \delta]}(s)$. The termination time $T = 1$ and $\Delta t = 0.2\Delta x^2$.

Δx	$\ u^\ell(x_i, t^n) - u_{\delta, \Delta x}^{qnl}(x_i, t^n)\ _{L_{\Omega \times [0, T]}^\infty}$	Order
$\frac{1}{50}$	0.04346549603691	—
$\frac{1}{100}$	0.030145239020954	0.527940440511889
$\frac{1}{200}$	0.027006661648969	0.158614852261122
$\frac{1}{400}$	0.026252371349129	0.040867570465478
$\frac{1}{800}$	0.026073054548579	0.009888136300599
$\frac{1}{1600}$	0.026032317322593	0.002255867438372

3.3 Robin Boundary Conditions Numerical Example

In this section, we repeat the process from the previous section, applying the same constraints, but now focusing on the nonlocal to local coupling with Robin boundary conditions. This analysis will explore how Robin boundary conditions, which combine both the function's value and its derivative at the boundary, affect the coefficient matrix and numerical solution.

Now we consider the Robin boundary value problem

$$\begin{cases} u_t(x, t) = \mathcal{L}^{qnl}u(x, t) + f(x, t) & x \in [-1, 1] \\ u(x, 0) = u_0(x) & x \in (-1, 1) \\ u_x(x, t) - u(x, t) = 0 & x \in \{-1\} \cup \{1\}. \end{cases}$$

This time, the Robin boundary conditions and definition of $u_x(x, t)$ give

$$u_x(x_1, t) - u(x_1, t) = 0 \tag{3.25}$$

which implies

$$\frac{u(x_2, t) - u(x_1, t)}{\Delta x} - u(x_1, t) = 0, \text{ or } (-1 - \Delta x)u_1 + u_2 = 0. \quad (3.26)$$

Similarly,

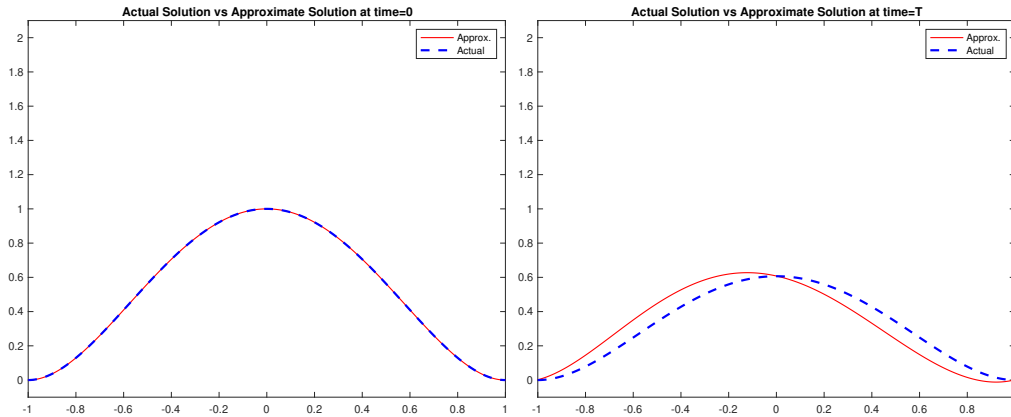
$$\begin{aligned} (-1 - \Delta x)u_2 + u_3 &= 0 \\ (-1 - \Delta x)u_3 + u_4 &= 0 \\ (-1 - \Delta x)u_4 + u_5 &= 0 \\ \dots &\dots \\ (-1 - \Delta x)u_{2N+r} + u_{2N+r-1} &= 0. \end{aligned} \quad (3.27)$$

Robin Boundary Condition Problem Numerical Example:

Let $N = 800$.

Exact Solution: $u(x, t) = (1 - x^2)^2 e^{-t}$

Force Function: $u_t = u_{xx} + f$, so $f(x, t) = -(1 - x^2)^2 e^{-t} - 4e^{-t}(3x^2 - 1)$



(a) solutions at $t = 0$

(b) solutions at $t = 1$

Figure 3.2: Numerical comparison between approximate and actual solution with Robin Boundary Conditions

Convergence with respect to Δx is not observed. The convergence order and $L^\infty_{\Omega \times [0, T]}$ differences between $u^\ell(x, t)$ and discrete solution of $u_{\delta, \Delta x}^{qnl}$ are listed in Table 3.2. Also the visual

comparison of the two solutions at $t = 0$ and $t = T$ are displayed in Figure 3.2 with good agreement.

Table 3.2: $L_{\Omega \times [0, T]}^\infty$ differences between the local continuous solution u^ℓ and discrete solution $u_{\delta, \Delta x}^{qnl}$. We fix $\delta = 3\Delta x$, and the kernel is $\gamma_\delta(s) = \frac{3}{\delta^3} \chi_{[-\delta, \delta]}(s)$. The termination time $T = 1$ and $\Delta t = 0.2\Delta x^2$.

Δx	$\ u^\ell(x_i, t^n) - u_{\delta, \Delta x}^{qnl}(x_i, t^n)\ _{L_{\Omega \times [0, T]}^\infty}$	Order
$\frac{1}{50}$	0.122199153334667	—
$\frac{1}{100}$	0.125828421422572	-0.042223537562521
$\frac{1}{200}$	0.124434138360483	0.016075485469575
$\frac{1}{400}$	0.122940268407174	0.017424801546374
$\frac{1}{800}$	0.121998183762725	0.011097869972930
$\frac{1}{1600}$	0.121478882814311	0.006154124078986

3.4 Boundary Conditions Conclusion

The results from the numerical examples using Dirichlet, Neumann, and Robin boundary conditions provide a clear comparison. The most accurate results are achieved with models that implement Dirichlet boundary conditions. In contrast, applying the LNL finite difference scheme with either Neumann or Robin boundary conditions does not yield approximations with strong convergence. The results for the Robin boundary condition example were particularly weaker compared to those with Neumann boundary conditions.

Neumann and Robin boundary conditions alter the continuous operator derived from energy variation. This suggests potential for future work, where modifications to the continuous model could account for these type of solutions, leading to more accurate approximations under Neumann and Robin boundary conditions. Despite these challenges, we still applied the finite difference scheme to approximate solutions with Robin boundary conditions to compare the outcomes across the different boundary types

REFERENCES

- [1] Burak Aksoylu and Michael L. Parks. Variational theory and domain decomposition for nonlocal problems. *Applied Mathematics and Computation*, 217(14):6498–6515, 2011.
- [2] Vesa Vuorinen Sergiy V. Divinski Alope Paul, Tomi Laurila. *Thermodynamics, Diffusion and the Kirkendall Effect in Solids*. Springer, 2023.
- [3] Fuensanta Andreu-Vaillo, Jose M. Mazon, Julio D. Rossi, and J.Julian Toledo-Melero. *Nonlocal diffusion problems*. Mathematical surveys and monographs ; v. 165. American Mathematical Society, Providence, R.I, 2010.
- [4] P. Bates and A. Chmaj. An integrodifferential model for phase transitions: Stationary solutions in higher space dimensions. *Journal of Statistical Physics*, 95:1119–1139, 1999.
- [5] F. Bobaru and M. Duangpanya. The peridynamic formulation for transient heat conduction. *International Journal of Heat and Mass Transfer*, 53:4047–4059, 2010.
- [6] Floran Bobaru and Monchai Duangpanya. The peridynamic formulation for transient heat conduction. *International Journal of Heat and Mass Transfer*, 53(19):4047–4059, 2010.
- [7] Allert Bruckmaier F, Neuling R, Littin N, Amrein P, and Briegel K S. Imaging local diffusion in microstructures using nv-based pulsed field gradient nmr. In *Cambridge: Cambridge Open Engage*, volume preprint, 2023.
- [8] A. Buades, B. Coll, and J. M. Morel. Image denoising methods. a new nonlocal principle. *SIAM Review*, 52(1):113–147, 2010.
- [9] Claudia Bucur and Enrico Valdinoci. *Nonlocal diffusion and applications*. Springer, 2016.
- [10] Ceren Budak, Divyakant Agrawal, and Amr El Abbadi. Diffusion of information in social networks: Is it all local? In *2012 IEEE 12th International Conference on Data Mining*, pages 121–130, 2012.
- [11] Emmanuel Chasseigne, Manuela Chaves, and Julio D. Rossi. Asymptotic behavior for nonlocal diffusion equations. *Journal de Mathematiques Pures et Appliquees*, 86:271–291, 2006.
- [12] Marta D’Elia, Xingjie Li, Pablo Seleson, Xiaochuan Tian, and Yue Yu. A review of local-to-nonlocal coupling methods in nonlocal diffusion and nonlocal mechanics. *To appear on Journal of Peridynamics and Nonlocal Modeling*, 2020.

- [13] Qiang Du, Max Gunzburger, R Lehoucq, and Kun Zhou. Analysis and approximation of nonlocal diffusion problems with volume constraints. *SIAM Review*, 56:676–696, 2012.
- [14] Qiang Du, Max Gunzburger, R Lehoucq, and Kun Zhou. A nonlocal vector calculus, nonlocal volume-constrained problems, and nonlocal balance laws. *Mathematical Models and Methods in Applied Sciences*, 23:493–540, 2013.
- [15] Qiang Du, Xingjie Helen Li, Jianfeng Lu, and Xiaochuan Tian. A quasinonlocal coupling method for nonlocal and local diffusion models. *SIAM Journal on Numerical Analysis*, 56:1386–1404, 2018.
- [16] Qiang Du and Robert Lipton. Peridynamics, fracture, and nonlocal continuum models. *SIAM News*, 47(3), 2014.
- [17] Qiang Du and Kun Zhou. Mathematical analysis for the peridynamic nonlocal continuum theory. *Mathematical Modelling and Numerical Analysis*, 45:217–234, 2010.
- [18] Marta DâElia, Qiang Du, Christian Glusa, Max Gunzburger, Xiaochuan Tian, and Zhi Zhou. Numerical methods for nonlocal and fractional models. *Acta Numerica*, 29:1–124, 2020.
- [19] M. Elices, G. V. Guinea, J. GÃmez, and J. Planas. The cohesive zone model : advantages, limitations and challenges. *Engineering Fracture Mechanics*, 69 : 137 – 163, 2002.
- [20] Paul Fife. Some nonclassical trends in parabolic and parabolic-like evolutions. In *Trends in Nonlinear Analysis*, pages 153–191. Springer, 2003.
- [21] Walter Gerstle, Nicolas Sau, and Stewart Silling. Peridynamic modeling of plain and reinforced concrete structures. *18th International Conference on Structural Mechanics in Reactor Technology (SMiRT 18)*, 2005.
- [22] Guy Gilboa and Stanley Osher. Nonlocal operators with applications to image processing. *Multiscale Modeling and Simulation*, 7(3):1005–1028, 2009.
- [23] Amanda Gute and Xingjie Li. Maximum principle preserving finite difference scheme for 1-d nonlocal-to-local diffusion problems. *Results in Applied Mathematics*, 12, 2021.
- [24] Y. D. Ha and F. Bobaru. Studies of dynamic crack propagation and crack branching with peridynamics. *International Journal of Fracture*, 162:229–244, 2010.
- [25] Y. D. Ha and F. Bobaru. Characteristics of dynamic brittle fracture captured with peridynamics. *Engineering Fracture Mechanics*, 78:1156–1168, 2011.
- [26] Siavash Jafarzadeh and Adam Larios. Efficient solutions for nonlocal diffusion problems boundary-adapted spectral methods. *Journal of Peridynamics and Nonlocal Modeling*, 2:85–110, 2020.
- [27] Dennis Kriventsov. Regularity for a local-nonlocal transmission problem. *Archive for Rational Mechanics and Analysis*, 217, 04 2014.

- [28] Xingjie Helen Li and Jianfeng Lu. Quasinonlocal coupling of nonlocal diffusions. *SIAM*, 2016. arXiv preprint arXiv:1607.03940.
- [29] Xingjie Helen Li and Jianfeng Lu. Quasi-nonlocal coupling of nonlocal diffusions. *SIAM Journal on Numerical Analysis*, 55(5):2394–2415, 2017.
- [30] Xingjie Helen Li and Jianfeng Lu. Quasinonlocal coupling of nonlocal diffusions. *SIAM*, 55, 2017.
- [31] Xingjie Helen Li and Mitchell Luskin. A generalized quasinonlocal atomistic-to-continuum coupling method with finite-range interaction. *IMA Journal of Numerical Analysis*, 32:373–393, 2011.
- [32] R. Lipton. Dynamic brittle fracture as a small horizon limit of peridynamics. *Journal of Elasticity*, 117:21–50, 2014.
- [33] R. Lipton. Cohesive dynamics and brittle fracture. *Journal of Elasticity*, 124:143–191, 2016.
- [34] Q. Ma, W. Li, J. Bortnik, R. M. Thorne, X. Chu, L. G. Ozeke, G. D. Reeves, C. A. Kletzing, W. S. Kurth, G. B. Hospodarsky, M. J. Engebretson, H. E. Spence, D. N. Baker, J. B. Blake, J. F. Fennell, and S. G. Claudepierre. Quantitative evaluation of radial diffusion and local acceleration processes during gem challenge events. *Journal of Geophysical Research: Space Physics*, 123(3):1938–1952, 2018.
- [35] Eduard Marusic-Paloka and Igor Pazanin. The robin boundary condition for modeling heat transfer. *Proceedings of the Royal Society A*, 480, 2024.
- [36] R. Kent Nagle and Edward B. Saff. *Fundamentals of Differential Equations*. Benjamin Cummings Publishing Company, Inc., second edition, 1989.
- [37] M. L. Parks, Richard B. Lehoucq, Steven J. Plimpton, and Stewart Silling. Implementing peridynamics within a molecular dynamics code. *Computer Physics Communications*, 179:777–783, 2008.
- [38] Lorenzo Rosasco, Mikhail Belkin, and Ernesto De Vito. On learning with integral operators. *Journal of Machine Learning Research*, 11(30):905–934, 2010.
- [39] Julio Rossi. Nonlocal diffusion equations with integrable kernels. *Notices of the American Mathematical Society*, September 2020.
- [40] H. L. Royden. *Real analysis [by] H. L. Royden*. Macmillan, New York, 2d ed. edition, 1968.
- [41] S.A. Silling and R.B. Lehoucq. Peridynamic theory of solid mechanics. *ScienceDirect*, 44:73–168, 2010.
- [42] Stewart Silling. Reformulation of elasticity theory for discontinuities and long-range forces. *Journal of the Mechanics and Physics of Solids*, 48:175–209, 2000.

- [43] Stewart Silling and R. B. Lehoucq. Peridynamic theory of solid mechanics. *Advances in Applied Mechanics*, 44:73–168, 2010.
- [44] Michael J. Steele. *Stochastic calculus and financial applications*. Springer, 2010.
- [45] Xiaochuan Tian and Qiang Du. Analysis and comparison of different approximations to nonlocal diffusion and linear peridynamic equations. *SIAM Journal on Numerical Analysis*, 51:3458–3482, 2013.
- [46] Xiaochuan Tian and Qiang Du. Asymptotically compatible schemes and applications to robust discretization of nonlocal models. *SIAM Journal on Numerical Analysis*, 52:1641–1665, 2014.
- [47] N. Trask, H. You, Y. Yu, and M. L. Parks. An asymptotically compatible meshfree quadrature rule for nonlocal problems with applications to peridynamics. *Computer Methods in Applied Mechanics and Engineering*, 343:151–165, 2019.
- [48] Jan TÅžnnesen, Sabina HrabÄtovÄj, and Federico N. Soria. Local diffusion in the extracellular space of the brain. *Neurobiology of Disease*, 177:105981, 2023.
- [49] M. Vynnycky. An asymptotic model for the formation and evolution of air gaps in vertical continuous casting. *Proceedings of the Royal Society A*, 465, 2009.
- [50] H. You, Y. Yu, and D. Kamensky. An asymptotically compatible formulation for local-to-nonlocal coupling problems without overlapping regions. *Computer Methods in Applied Mechanics and Engineering*, 366, 2020.